13

# Macromolecular Crystallization Controlled by Colloidal Interactions: The Case of Urate Oxidase

Françoise Bonneté
*Institut des Biomolécules Max Mousseron,*
*Université d'Avignon et des Pays de Vaucluse*
*France*

## 1. Introduction

Crystallization is a natural or artificial process involving the physical transformation of a fluid or a gas into a regularly organized solid form, the crystal (Fig.1). It occurs in many fields such as health sciences, geosciences, microelectronics, industrial chemical processes.

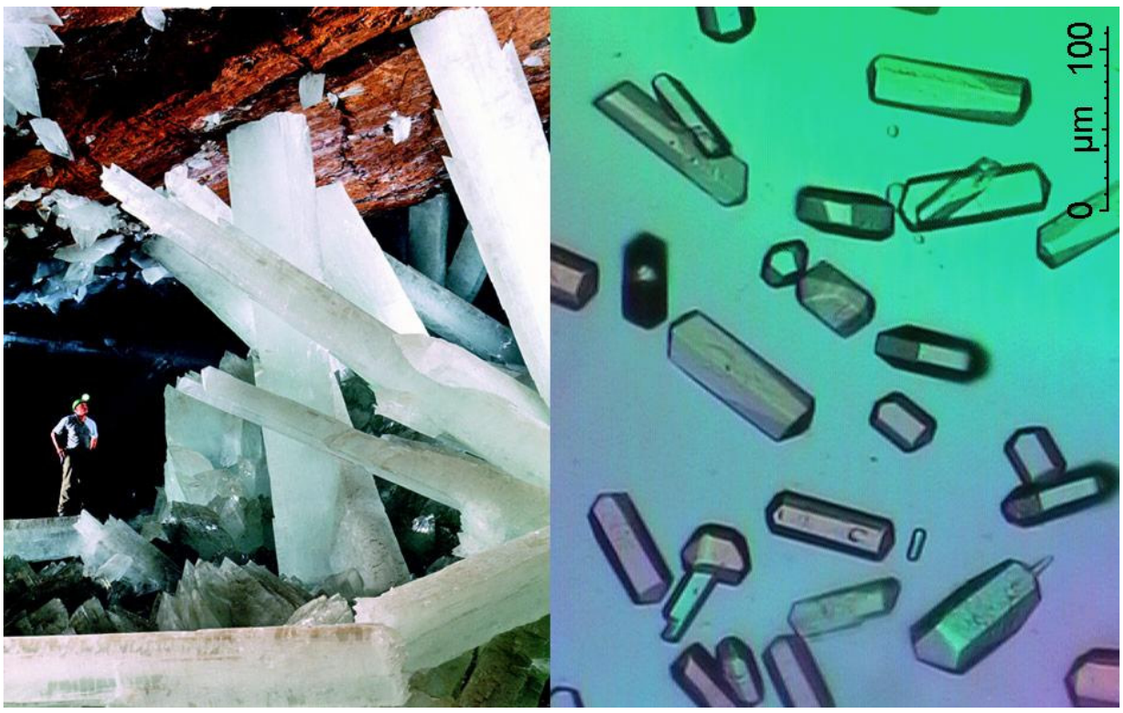


Fig. 1. (Left) Giant Crystal Cave's Mystery Solved (Lovgren, 2007); (Right) Micrometric protein crystals in batch of a therapeutic enzyme, Urate oxidase.

In health sciences, crystals can grow *in vivo* or *in vitro*. *In vivo* this can be due to pathologies (Pande et al., 2001); *in vitro*, crystallization is mainly used to decipher 3D atomic structures

of biological macromolecules and understand their structure-function relationship. Originally, crystallization was a method of purification (Sumner, 1926), but now chromatography has replaced protein crystallization in the protein purification process. Today, crystallization is still used for purification and formulation steps in the biotechnology and pharmaceutical industries (Weber et al., 2008). It is a powerful and economical protein purification method, since high-purity proteins can be obtained in a single-step operation. However, crystallization remains an empirical process, still based on trial-and-error methods using commercial crystallization cocktails. Crystallization for protein purification is not always practical, since it requires good knowledge of the phase diagram and a substantial quantity of the protein to be crystallized. Although proteins are composed of amino acids of limited types, their structural diversity makes their crystallization conditions difficult to predict. Crystallization conditions include a wide spectrum of parameters such as pH and buffer type, ionic strength, type and concentration of precipitant, temperature, presence and concentration of surfactant molecules and other additives (e.g. cofactors, inhibitors) and, above all, protein concentration. Finding an efficient method to easily crystallize any protein has been, and can be expected to continue to be, a major challenge. Many methods of protein crystallization have been described (Bergfors, 2009). Since the advent of structural genomic programs, a lot of work has been done on automation and miniaturization of crystallization methods in view of the limited amount of protein material available, particularly membrane proteins. Other methods that limit convection effects on crystal growth have shown their efficacy on diffraction quality: crystallization in microgravity (McPherson et al., 1999), in gels (Ng et al., 2003), in microfluidics (Zheng et al., 2005) and other unconventional methods (Sazaki et al., 2004). All these general crystallization methods have recently been thoroughly reviewed (Sauter et al., 2011). But crystallization is not restricted to certain methodologies. Crystallization is a physical process, which consists of two major distinct but inseparable events, nucleation and growth, governed by both thermodynamic and kinetic factors. A pre-nucleation step can be added, creating a supersaturation state. For a long time it was thought that crystallization obeys no comprehensive theory. In the 80's-90's, rational and physical approaches were developed to understand the fundamentals of nucleation and crystal growth of proteins. The concepts of nucleation and crystal growth were described (Feher & Kam, 1985) and recently reviewed (Chernov, 2003; García-Ruiz, 2003). While growth of macromolecular crystals is well characterized, in particular by direct visualization using atomic force microscopy, there are fewer studies of nucleation, since it requires high supersaturation, that is to say often high concentrations of proteins. Some nucleation studies were performed with a model protein such as lysozyme by dynamic light scattering (Mikol et al., 1989) or small angle X ray (Finet et al., 1998) or neutron scattering (Boué et al., 1993) in order to understand the prenucleation and nucleation steps. This was the beginning of the development of rational approaches based on an understanding of the physical properties of macromolecular solutions. Numerous articles and reviews examined the correlation between crystallization and interactions between macromolecules in solution (Ducruix et al., 1996; Muschol & Rosenberger, 1995), applicable to soluble proteins like membrane proteins (Hitscherich et al., 2000). The measurement of the second virial coefficient, noted indifferently $A_2$, $B_2$ or $B_{22}$ depending on the authors, appeared to be a powerful tool for predicting crystallization conditions (George & Wilson, 1994). George & Wilson showed that a restrictive range of values of the second virial coefficient was

favorable to crystallization of soluble proteins. This "crystallization slot", which is about [-1x10$^{-4}$; -8x10$^{-4}$ mol.mL.g$^{-2}$], corresponds to slight or moderate attractions. Second virial coefficients can be measured using different experimental techniques, including osmotic pressure (Haynes et al., 1992), static light scattering (SLS) (Velev et al., 1998), ultracentrifugation (Behlke & Ristau, 1999), small-angle X-ray scattering (SAXS) (Bonneté et al., 1999), small-angle neutron scattering (SANS) (Gripon et al., 1997), size-exclusion chromatography (Bloustine et al., 2003) and self-interaction chromatography (SIC) (Tessier et al., 2002). Studying different biological macromolecules (protein, virus) of various sizes, molecular masses or net charge (Bonneté & Vivares, 2002), we showed that a dimensionless second virial coefficient normalized to protein excluded volume gave a better representation of the effective pair potential between macromolecules (McQuarrie, 2000) when comparing the effects of physico-chemical parameters leading to crystallization. We found a new dimensionless crystallization slot [-10; 3] in which the Brome mosaic virus (BMV) (Casselyn et al., 2001) was found to crystallize with a slightly positive second virial coefficient $a_2$ = +2.8. This $a_2$ value was not inconsistent with attractive interactions since the dimensionless second virial coefficient of a pure hard-sphere potential is equal to 4. Indeed the effective pair potential of biomolecules in solution is the sum of different components including, in particular, hard sphere repulsion, van der Waals attraction, electrostatic effects and depletion attraction. Phase diagrams of biological macromolecules are therefore governed by an appropriate combination of these interaction potentials in solution. Repulsive regimes favor solubility, whereas the presence of attractive potentials may induce a variety of phase transitions, including the desired macromolecular crystallization. These pair potentials are medium range, from a few Å up to tenths of Å, and each of them is under separate control of physico-chemical conditions such as pH, temperature and solvent composition (Hansen & McDonald, 1976; Israelachvili, 1994). The desired fine tuning of the interactions for controlled crystallization requires identifying the individual contributions. In order to do so, theoretical simulations were performed on series of SAXS scattered intensities recorded on hen egg white lysozyme as a function of pH, salt concentration, salt type and temperature, on alpha crystallins (Finet & Tardieu, 2001) and urate oxidase (Vivares et al., 2002) as a function of polyethylene glycol (PEG). In this chapter we will show, using the example of urate oxidase, how to choose physico-chemical conditions, how they control the different interaction forces and how these forces can be modulated to design different phase diagrams for different applications (biocrystallography, or pharmaceutical processes for example).

## 2. Theoretical and experimental background

It is common practice in the colloid field to calculate phase diagrams from interaction potentials in solution (Asherie et al., 1996). The forces between colloids in solution include hard sphere repulsion plus attraction, whose range may modify the appearance of the phase diagram (Fig.2). In a colloid-polymer mixture, the presence of stable or metastable phase transitions can be determined by the ratio of the attraction range and the colloid size (Lekkerkerker, 1997), the range of the attractive interaction between colloids in solution being controlled by the size of the polymer (Poon, 2002). Predicting the phase diagrams of proteins based on knowledge of interaction forces may therefore be a more effective alternative for controlled crystallization than trial-and-error screenings.

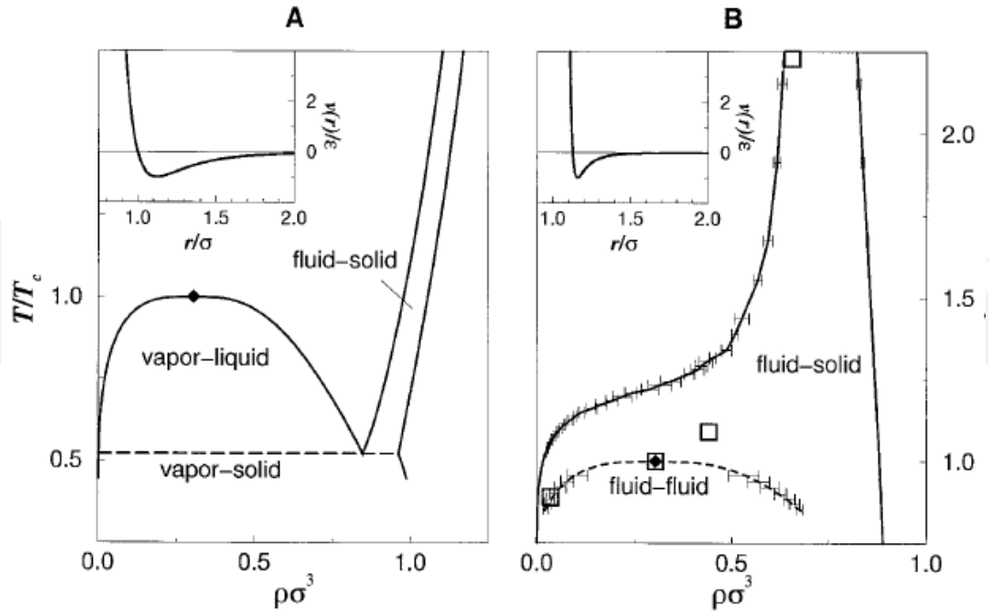


Fig. 2. Typical phase diagram of colloids A) with long-range attraction; B) with short- range attraction (ten Wolde & Frenkel, 1997)

Thus, a thorough understanding of the interaction potentials that govern protein phase diagrams will allow better control of crystal growth. The good news is that this can be applied successfully to biomacromolecule crystallization. The phase diagram of biomacromolecules, usually represented by the solubility curve, is governed by an appropriate combination of interaction potentials (Tardieu et al., 1999). Repulsion favors solubility, whereas attractions induced either by salt or polymer addition favor phase transitions, including crystallization. Ideally, to grow crystals, interaction potentials would be calculated in solution from knowledge of the macromolecule's characteristics, i.e. sequence, molecular mass, charge and isoelectric point as a function of physico-chemical environment (pH, temperature, ionic strength, etc.), leading to its phase diagram. Alas, this is not yet possible. However, using knowledge of the physico-chemical and biochemical characteristics of macromolecules in solution, we can choose relevant parameters to modulate potential forces and control nucleation rate and crystal growth. While it is not yet possible to calculate interaction potentials from macromolecule characteristics, it is possible experimentally to measure the resulting interactions in solution, either repulsive or attractive, through second virial coefficient ($A_2$) measurements, and then to simulate the underlying pair potentials. $A_2$ can be measured from the macromolecule concentration dependence of different experimental measurements, such as osmotic pressure, analytical ultracentrifugation, self-interaction chromatography, static light scattering, small angle X-ray or neutron scattering (SAXS or SANS). We used SAXS because it offers additional advantages. By combining SAXS measurements and numerical simulations, we can also analyze forces present in macromolecule solutions, that is to say the different repulsive and attractive components, and study them as a function of common physico-chemical parameters. This type of approach has already been used in the case of colloid-polymer mixtures (Lutterbach et al., 1999a; Lutterbach et al., 1999b; Ye et al., 1996) or biopolymers (Malfois et al., 1996; Vérétout et al., 1989).

### 2.1 Small Angle X-ray scattering and numerical calculation

To analyze the interaction potentials that control phase diagrams, we combined SAXS and numerical simulations. The total normalized intensity I(c,q), scattered by a solution of monodisperse spherical particles at a scattering angle 2θ, can be expressed as a function of the particle concentration c and the modulus of the scattering vector q, $q = 4\pi\lambda^{-1}\sin\theta$ (note that $q = 2\pi s$*) by:

$$I(c,q) = I(0,q) \times S(c,q) \tag{1}$$

I(0,q) is the intensity scattered by one particle and is usually called the particle form factor. Experimentally, the form factor is generally obtained from curves recorded at low concentrations to avoid interaction effects. The form factor gives information on the particle shape and its oligomeric state. At low angles, the form factor of an ideal solution ($c \to 0$, without interaction) can be written:

$$I(c \to 0, q) = I(c \to 0, 0).\exp\left(-\frac{R_g^2}{3}q^2\right) \tag{2}$$

Similarly, for non-ideal solutions, the low angle part of the intensity curves recorded as a function of c is written:

$$I(c, q) = I(c, 0).\exp\left(-\frac{R_g^2}{3}q^2\right) \tag{3}$$

Therefore a « Guinier plot », i.e. a Ln I(q) plot versus $q^2$ (Guinier & Fournet, 1955), provides, with intensity at the origin, I(0,0) or I(c,0), and with the structure factor at the origin, S(c,0), since S(c,0)=I(c,0)/I(0,0). Indeed, with interacting spherical particles, departure from ideality can be accounted for by the interference term, S(c,q), usually called the solution structure factor. The value of S(c,q) at zero-q angle gives information on the nature of interactions between particles. With repulsive interactions, the particles are evenly distributed and S(c,0) is lower than 1 (Example Fig. 3A). With attractive interactions, fluctuations in particle distribution are observed and S(c,0) is larger than 1. The nature of the net interactions, either attractive or repulsive, can easily be determined by the plot of the structure factor at the origin, S(c,0), as a function of particle concentration, since it is related to the osmotic with pressure Π by:

$$S(c,0) = \frac{RT}{M}\left(\frac{\partial \Pi}{\partial c}\right)^{-1} \tag{4}$$

With

$$\frac{\Pi}{cRT} = \frac{1}{M} + A_2 c + A_3 c^2 + \ldots \tag{5}$$

the concentration c being expressed in $g.cm^{-3}$.

*Note: Depending on SAXS beamlines used for experiments, the scattered intensity was expressed either as a function of $q = 4\pi\lambda^{-1}\sin\theta$ or $s = 2\lambda^{-1}\sin\theta$ in $Å^{-1}$ or $nm^{-1}$

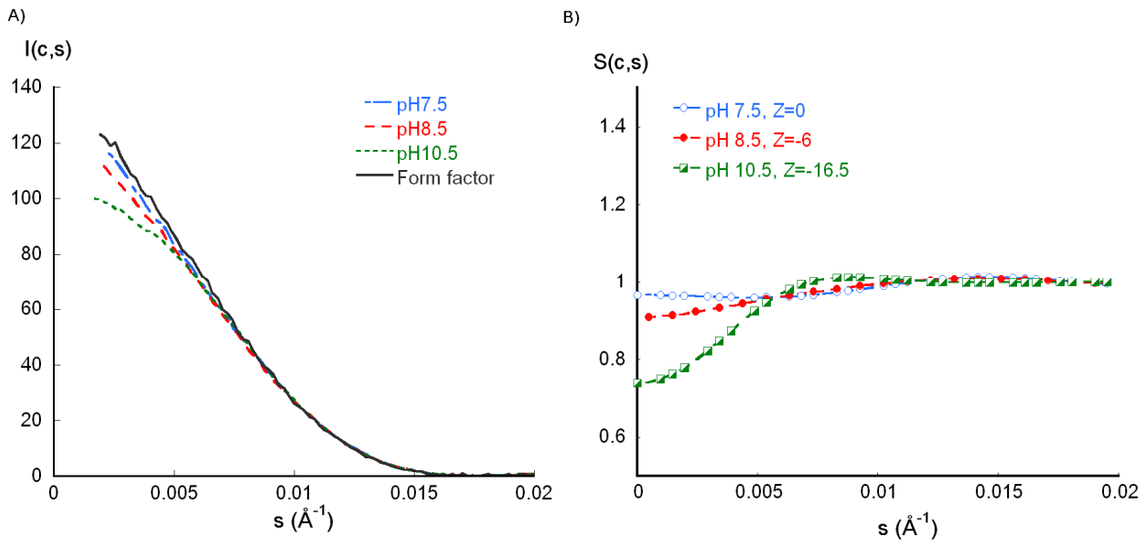


Fig. 3. A) Scattering intensities of urate oxidase as a function of pH. B) Experimental (dots) and fitted (lines) repulsive structure factor of urate oxidase at different pH corresponding to repulsive interactions, S(c,0) < 1.

Therefore, the second virial coefficient can be obtained by the expression:

$$S(c,0) = \frac{I(c,0)}{I(0,0)} = \frac{1}{1 + 2.M.A_2.c + \ldots} \tag{6}$$

Experimentally the structure factor can be obtained by intensity extrapolation from the expression:

$$S(c,0) = \frac{\lim_{q \to 0} I(c,q)}{\lim_{c \to 0} I(c,0)} \tag{7}$$

The slope of the linear fit gives the coefficient $A_2$ in mol.ml.g$^{-2}$.

$$S(c,0) \approx 1 - 2.M.A_2.c \tag{8}$$

If $A_2$ is positive, the overall interactions are repulsive (Example Fig. 3B); if $A_2$ is negative, the interactions are attractive.

The solution can be described mathematically as the convolution product of a particle shape and a particle distribution. $S(c,q)$ is the Fourier transform of the spherically averaged auto-correlation function $g(r)$ of the particle distribution or pair-distribution function:

$$S(c,q) = 1 + \rho \int 4\pi r^2 (g(r) - 1) \frac{\sin rq}{rq} dr \tag{9}$$

where $\rho = cN_a/M$ is the number density of particles, i.e. the number of particles per unit volume and $c$ is the particle concentration in g.cm$^{-3}$. Models and numerical methods based

on statistical mechanics are extended to proteins in solution (Lomakin et al., 1996; Malfois, et al., 1996). Calculation of structure factors is based on models of pair particle potential $U(r)$, from which a particle distribution $g(r)$ at equilibrium is inferred. The calculation of $g(r)$ is based on the Ornstein-Zernike (OZ) equation and on the hypernetted chain (HNC) integral equation and uses an iterative method (Belloni, 1985; 1988). For one-component fluids, the OZ relationship between total, $h(r) = g(r) - 1$, and direct, $c(r)$, correlation functions is written in Fourier space (where FT indicates a Fourier transform, normalized by the density ρ):

$$S(c, q) = 1 + \mathrm{FT}h(r) = 1/(1/\mathrm{FT} - c(r)) \tag{10}$$

If we introduce an auxiliary function $\gamma(r) = h(r) - c(r)$, the integral HNC equation is:

$$g(r) = \exp[-\beta U(r) + \gamma(r)] \tag{11}$$

where $U(r)$ is the interaction pair potential. To numerically solve the OZ equation with the above closure relation, iterations are used. The structure factor $S(c,q)$, and/or macroscopic properties and thermodynamic variables, are then calculated from the Fourier transform and integrals of pair distribution function $g(r)$ (Hansen & McDonald, 1976). The calculated structure factor is then compared to the experimental structure factor as shown in an example Fig. 3B.

For the simplest "one component" model, only the interaction pair potentials between macromolecules, which interact through solvent and ions, are explicitly considered in the numerical simulations. Since in such calculations the exact potential shape is not critical, we describe the potentials, either attractive or repulsive, in the mathematical form of a Yukawa potential, which is a function of three parameters, hard sphere diameter, σ, depth (strength), J, and range, d, according to:

$$U(r)/k_B T = J\,(\sigma/r)\,\exp[-(r-\sigma)/d] \tag{12}$$

In the case of binary mixtures of macromolecules (mac) and polymers (pol) i.e. of "two component" systems, the total scattered intensity, $I(c_i c_j,q)$, can be expressed as a function of component concentrations $c_i$ by (Belloni, 1991):

$$\begin{aligned} I\left(c_i c_j, q\right) &= \Sigma_i \Sigma_j \sqrt{c_i c_j}\, \sqrt{I_i\left(0,q\right) I_j\left(0,q\right)} S_{ij}\left(q\right) \\ &= I_{mac}\left(c_{mac}, q\right) + I_{mac-pol}\left(c_{mac}, c_{pol}, q\right) + I_{pol}\left(c_{pol}, q\right) \end{aligned} \tag{13}$$

Because of the presence of a cross term, only SAXS intensities and not structure factors can be compared. The polymer form factor $I_{pol}(0,q)$ can be taken as equal to the Debye form factor, which is valid for a Gaussian coil and has already been used successfully with PEG (Debye, 1946):

$$I_{pol}(0,q) = I_{pol}(0,0)\,(2/x^2)\,(\exp(-x) - 1 + x) \tag{14}$$

where $x = q^2 R_g^2$, and $R_g$ is the polymer radius of gyration. Partial structure factors $S_{ij}(q)$ are related to the Fourier transform of partial pair distribution function $g_{ij}(r)$:

$$S_{ij}(q) = \delta_{ij} + \sqrt{c_i c_j} \int (g_{ij}(r) - 1) \exp(irq)\, dr \tag{15}$$

where i,j = 1,2, $\delta_{ij}$ is the Kronecker symbol ($\delta_{ij}$=0 when i≠j and $\delta_{ij}$=1 when i=j) and r the interparticle distance. To determine the pair distribution function, the usual procedure, as for one component systems, is to use the Ornstein-Zernike equation to link the total, $h_{ij}(r) = g_{ij}(r) - 1$, and the direct, correlation $c_{ij}(r)$ functions. The closure equation is once again the HNC equation. From a set of the three direct potentials, $U_{pol\text{-}pol}(r)$, $U_{mac\text{-}pol}(r)$ and $U_{mac\text{-}mac}(r)$, the theoretical scattered intensity from the binary mixture can be calculated and compared to the experimental scattering curve (Vivares, et al., 2002).

## 2.2 Direct pair potentials

### 2.2.1 The DLVO model

The direct protein-protein potential $U_{uox\text{-}uox}(r)$ was chosen equal to the DLVO potential. We had already successfully applied the DLVO model to different proteins at low-salt concentrations (Malfois, et al., 1996; Tardieu, et al., 1999). The DLVO potential is the sum of three potentials: a hard-sphere potential, an electrostatic repulsion and a van der Waals attraction. The hard-sphere potential reflects the fact that proteins cannot interpenetrate, the repulsive coulombic potential is due to the fact that each protein holds the same net charge and the van der Waals attractive potential is the resulting dispersion interaction between proteins. For the sake of simplicity, we chose a Yukawa shape for the coulombic and the van der Waals potentials, a Yukawa shape van der Waals potential having been shown to be sufficient to describe the attractive protein-protein interaction in aqueous solutions.

Respective mathematical expressions of the three potentials are described:

- Hard-sphere potential:

$$\begin{aligned} U^{HS}_{UOX-UOX}(r) &= +\infty \quad r \le \sigma \\ &= 0 \quad r > \sigma \end{aligned} \tag{16}$$

with σ the protein diameter

- Repulsive coulombic potential:

$$U^{coul}_{UOX-UOX}(r) = Z^2 L_B / [\sigma(1+0.5\sigma/\lambda_D)^2].(\sigma/r).\exp(-(r-\sigma)/\lambda_D) \quad r > \sigma \tag{17}$$

with Z the effective protein charge, $L_B$ the Bjerrum length (equal to $e^2/(4\pi\varepsilon_0\varepsilon_s k_B T) = 7.31$Å at T = 293.15K with $\varepsilon_s = \varepsilon_{H2O} = 80$) and $\lambda_D$ the Debye length ($\lambda_D(\text{Å}) = 3/\sqrt{I}$ at 293.15 K where I is the ionic strength expressed in mol/l). The potential is expressed in $k_BT$ units.

Repulsive interactions are expected to vary with pH and to be screened with ionic strength (addition of alcohol, which reduces the water dielectric constant, can also reduce the repulsion).

- van der Waals potential:

$$U^{VdW}_{UOX-UOX}(r) = -J_{VdW}.(\sigma/r).\exp(-(r-\sigma)/d) \quad r > \sigma \tag{18}$$

with $J_{VdW}$ (in $k_BT$ units) and d (in Å), respectively, the depth and the range of the potential.

In practice, the van der Waals component is determined at or close to the pI. With small compact proteins, the best fit parameter for depth with a 3Å range was indeed found to be close to the calculated values, 2-3 $k_BT$ (Tardieu, et al., 1999) and the attraction was found to increase with decreasing temperature.

In the DLVO potential, hard-sphere and electrostatic interactions have a repulsive effect which favors solubility. Except possibly at pI, the van der Waals forces are weaker than the coulombic interactions (or even disappear). However, it is clear that the basic interactions considered in the DLVO potential model are generally unable to provide the attraction necessary for macromolecular nucleation and crystal growth. Fortunately, other forces can play a role.

### 2.2.2 The Hofmeister effect

Salt has long been known to act as a crystallizing agent (Arakawa & Timasheff, 1985). A number of phase diagrams were measured, e.g. by the Ducruix group (Carbonnaux et al., 1995; Guilloteau et al., 1992) and showed that solubility varies with the type of monovalent salt, following the direct/reverse order of the Hofmeister series according to whether the particles are studied at a pH higher/lower than the pI, respectively.

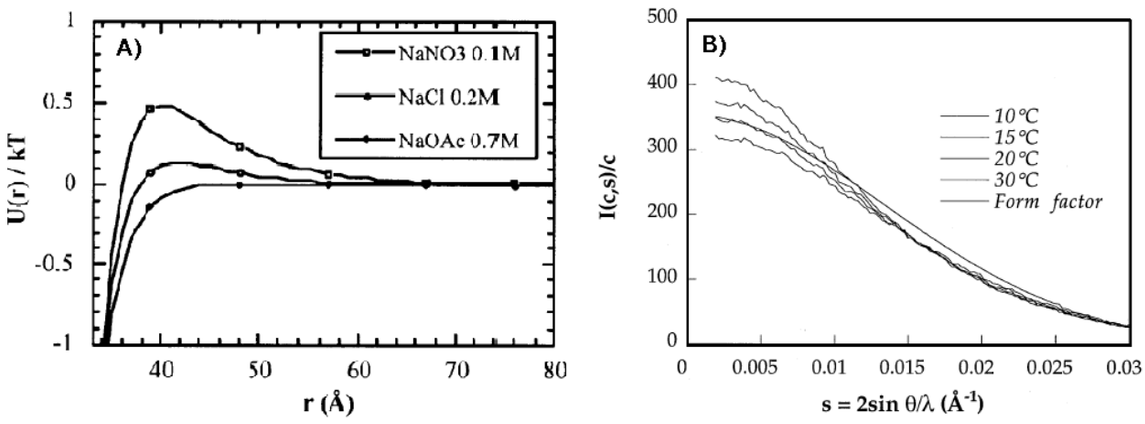


Fig. 4. A) Interaction potential of lysozyme in different salts. B) Normalized scattering intensity of Lysozyme in NaCl 200 mM pH 4.5 at different temperatures (curves in the same order as in legend for both figures).

When the effect of monovalent salts on protein interactions in solution was analyzed (Muschol & Rosenberger 1995, Tardieu *et al*., 1999), whatever the particle size , at medium ionic strength (> 0.2 M), monovalent anions were observed not only to screen the charges, but to induce an additional attraction, specific to salt type (Finet et al., 2004). This attraction is short-range, about 3Å, and increases with decreasing temperature.

### 2.2.3 Depletion attraction

The addition of neutral non-interacting polymers to colloidal solutions has long been known to induce a depletion attraction (Asakura & Oosawa, 1954). This depletion interaction can be explained in a simplified manner for an ideal polymer solution.

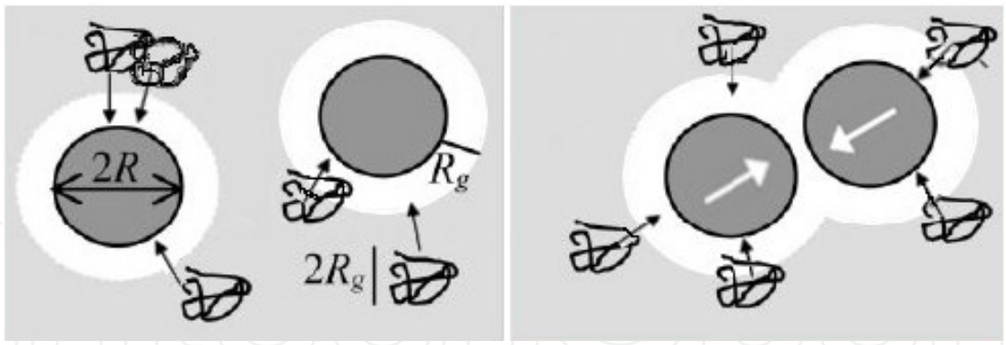


Fig. 5. Schematic illustration of the depletion effect in a colloid-polymer mixture

Molecules of polymer - characterized by their radius of gyration $R_g$ - and colloids cannot mutually interpenetrate, and furthermore, the center of polymers is excluded from a region of thickness $R_g$ around each colloidal particle. This excluded volume is called the depletion zone. When two colloid particles come sufficiently close to each other, their depletion zones overlap and the free volume accessible to the polymer molecules increases, leading to a gain in entropy of the system. Thermodynamically, it is therefore more favorable for the polymer when colloidal particles approach each other, i.e. when there is an attractive interaction between them. This model remains valid as long as polymer molecules do not overlap. To describe the direct polymer-polymer potential $U_{pol\text{-}pol}$ (r), we used an approach where the effective potential is finite for all distances between two polymer molecule centers of mass. Molecules of polymer were therefore considered as "soft colloids". The mathematical form chosen for the polymer-polymer potential was a Gaussian form (Bolhuis et al., 2001):

$$U_{pol-pol}(r) = J_{pol}.\exp(-(r / R_{pol})^2) \tag{19}$$

Where $J_{pol}$ (in $k_BT$ units) and $R_{pol}$ (in Å) are the prefactor parameter and the range of the Gaussian potential respectively.

For the direct protein-polymer potential $U_{pol\text{-}col}(r)$, we chose a Yukawa form, which depends on only two parameters:

$$\begin{aligned} U_{pol-col}(r) &= +\infty \; r \le \sigma / 2 \\ &= J_{pol-col} \cdot \frac{\sigma}{2r}.\exp(-(r-\sigma/2)/d_{pol-col}) \; r > \sigma / 2 \end{aligned} \tag{20}$$

with $J_{pol\text{-}col}$ (in $k_BT$ units) and $d_{pol\text{-}col}$ (in Å) the intensity and the range of the potential respectively.

Thus, the numerical simulations provide us with an effective macromolecule-macromolecule potential, $U^{eff}_{col\text{-}col}(r)$, which may be written as the sum of the macromolecular interaction potential in the absence of polymer, $U_{uox\text{-}uox}(r)$, and of the depletion term, $U_{depletion}$ (r):

$$U^{eff}_{col\text{-}col}(r) = U_{col\text{-}col}(r) + U_{depletion}\,(r) \tag{21}$$

The depletion potential is therefore obtained from equation 21. From numerical simulations performed on the binary mixture, urate oxidase-polyethylene glycol (Vivares, et al., 2002),

we found that the depth and the range of the effective potential increases with the addition of polymer.

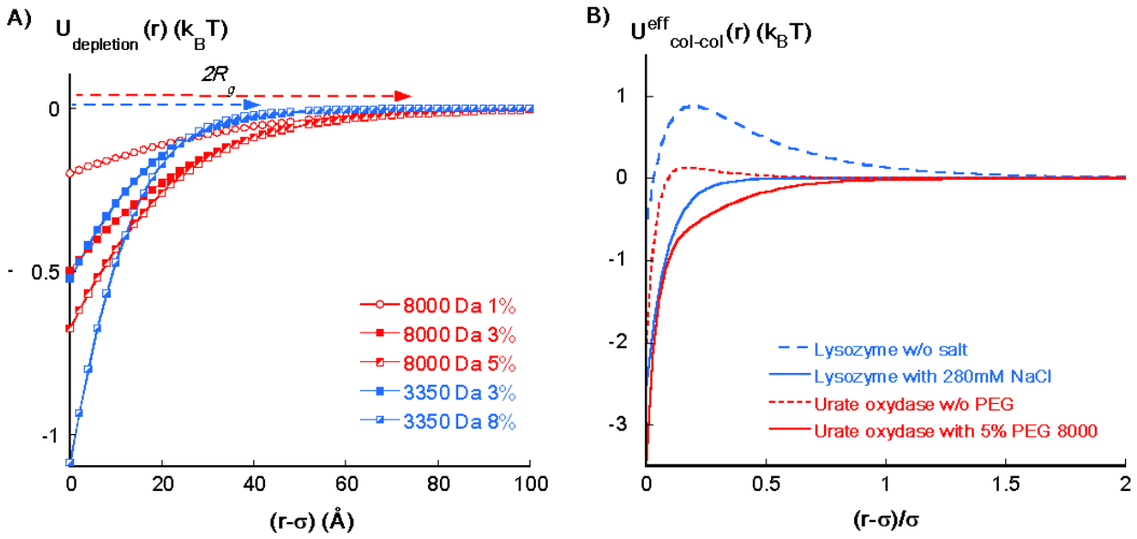


Fig. 6. A) Resulting depletion potential at different PEG concentrations for PEG 8000Da and PEG 3350Da; B) Comparison of the attractive potential induced by salt in lysozyme solutions and by PEG in urate oxidase solutions normalized to the particle diameter.

While depletion potential depth increases with polymer concentration whatever the polymer size, depletion range is approximately equal to $2R_g$ for each polymer, whatever the polymer concentration (Fig. 6A). Crystallization in polyethylene glycol is thus induced by a medium-range attractive potential between macromolecules, in addition to the short-range van der Waals. This result appears in contrast to that observed with small proteins like lysozyme, where crystallization was found to be induced by short-range attraction. The attractive potential range necessary for protein crystallization increases with the size of the macromolecule. In fact, it is interesting to note that, when normalized to the particle diameter, the salt- and PEG-induced interaction potentials that promote the crystallization of lysozyme (14300 Da) and urate oxidase (135000 Da) respectively are quite similar (Fig. 6B). Finally, since salt induces a short-range attraction and since polymer-induced potential range varies both with polymer size and with polymer concentration, by choosing salt in the Hofmeister series as well as polymer concentration and size it is possible to modify the phase diagram and thus control protein crystallization.

Nucleation and crystal growth are inseparable events, both of which depend on supersaturation. The nucleation step controls the structure of the crystalline phase and the number of crystals. Recently, it has been shown that interaction potentials play a key role in the determination of nucleation kinetic parameters (Bhamidi et al., 2005). Depending on the application (biocrystallography, powder diffraction, purification, for example), it appears important to control the nucleation step, supersaturation and, therefore, solubility.

We have seen that, whatever the salt or polymer used, macromolecular crystallization occurs in the presence of an attractive pair potential. We have analyzed how attraction and

repulsion can be varied by changes in the environment: pH, ionic strength, type of salt, polymers, and temperature (Tardieu, et al., 1999; Vivares, et al., 2002). With low molecular weight proteins, a coulombic, pH-dependent, repulsive potential plus a short-range, possibly van der Waals, attraction are sufficient to account for the behavior observed at low ionic strength. At higher ionic strengths, salt-specific effects following the (direct or reverse) order of the Hofmeister series correspond to an additional short-range salt-specific attraction. With increasing protein size, the van der Waals contribution becomes negligible. Adding polymers like polyethylene glycol (PEG) induces a depletion attraction. The way forward in growing crystals is therefore a fairly simple extension of these observed effects. While this path is not guaranteed to lead to success, it may well enable us to reduce the time and effort spent on trial-and-error methods.

## 3. A protein of pharmaceutical interest: Urate oxidase

Lysozyme has long been the model protein most often chosen to study nucleation and crystal growth mechanisms (Drenth, 2005; Gavira & Garcia-Ruiz, 2009; Liu et al., 2010; Vekilov, 2010), since it is easily available at low cost. We used urate oxidase from *Aspergillus flavus* as a new model system to explore the crystallogenesis of proteins in general and the crystallographic structure of urate oxidase in particular. Urate oxidase is used as a protein drug to reduce toxic uric acid accumulation and to treat the hyperuricemic disorders occurring during chemotherapy. Urate oxidase *from Aspergillus flavus* is produced, purified and made commercially available by Sanofi-Aventis (France). Urate oxidase is normally purified using multiple steps of concentration and chromatography (McGrath & Walsh, 2005). Like other proteins (Jacobsen et al., 1998), it could, however, be purified by crystallization (Giffard et al., 2011). Crystallization has the inherent advantages of providing higher final purity yields, not denaturing the protein of interest and often providing some stabilization effects, but it requires a good knowledge of the phase diagram and a substantial amount of the protein to be crystallized. The structure of the urate oxidase from *A. flavus* has been solved in the absence (Retailleau et al., 2004) as well as in the presence of different inhibitors (Retailleau et al., 2005). It is a homotetrameric enzyme of 135kDa with a subunit consisting of 301 amino acids. Although different urate oxidase structures have been determined, its catalytic mechanism is still poorly understood. One possible mechanism for the oxidation of uric acid could be revealed by the precise protonation state of the substrate during the reaction. Neutron crystallography can provide such information and make possible direct determination of the protonation states of the active site residues and substrate analogues (Oksanen et al., 2009). For this purpose, it is necessary to grow large, well ordered, deuterated crystals; here too, therefore, a good knowledge of the phase diagram is required. Finally, whether crystallization is aimed at urate oxidase purification or at growing highly diffracting crystals, a good knowledge of the phase diagram and thus of crystallization conditions are required. We used urate oxidase, then, as a model system both from a fundamental and an applied point of view, in suitable biological and physicochemical conditions, to characterize, simulate and modulate pair potentials present in solution and design appropriate phase diagrams for specific applications. We will show in particular, how macromolecule properties – such as sequence, molecular mass, isoelectric point, stability – can provide the parameters to be screened to obtain adequate phase diagrams.

## 4. Urate oxidase interactions in solution and implications for crystallization

The stability of urate oxidase from *Aspergillus flavus* was studied by differential scanning calorimetry (DSC) (Bayol et al., 1995) in conjunction with enzymatic activity measurement and size exclusion chromatography. The recombinant urate oxidase is not stable below pH 6 and shows maximum stability between pH 7.25 and 9.5 up to 35 °C. Studies of crystallization were therefore performed at a pH above 7.2 and a temperature below 35 ° C. pH 8 was identified as the value around which the enzyme stabilization activity is optimized (Aleman et al., 1998). The buffer selected for use is a sodium phosphate buffer at pH 8 at a concentration of between 5 mM and 100 mM. It was in this range of urate oxidase stability that different parameters (pH, nature of buffer, temperature, ionic strength, additives) were studied for their effects on interaction forces and their influence on phase diagrams.

### 4.1 pH and Salt effects

Urate oxidase is a large tetrameric enzyme of 135 kDa stable at pH above 7. Its theoretical isoelectric point (pI), calculated from its primary structure and the pKa of each charged amino acid, is 7.5 (Fig 7), consistent with IEF experiments.

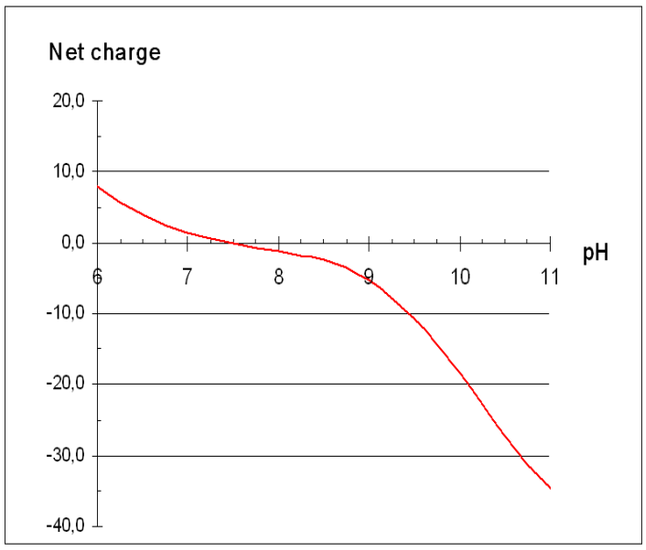


Fig. 7. Urate oxidase net charge as a function of pH

By definition, at pI without any other crystallizing agents, the protein net charge is zero. Thus, there is no electrostatic repulsion. The van der Waals attraction may therefore induce instability and aggregation of proteins. Usually protein solubility is minimum at pI (Riès-Kautt & Ducruix, 1999). At pH above pI, the urate oxidase negative net charge increases as pH increases. We therefore expect urate oxidase electrostatic repulsions to increase as the net charge increases.

A compilation of second virial coefficient ($A_2$) values of urate oxidase as a function of pH, determined from previous SAXS experiments (Giffard et al., 2008; Vivares & Bonneté, 2002) (Fig. 8A), shows that $A_2$ is positive whatever the pH above pI, as expected for repulsive interactions, and increases as both pH and protein net charge increase. However, as pH

approaches pI, $A_2$ remains positive, which is not consistent with pure van der Waals attraction at pI. This may be due to residual charges on the protein. In contrast, for a negative second virial coefficient measured in Tris buffer pH 8 close to pI without addition of salt (Fig. 8B), the second virial coefficient increases, becoming positive as salt concentration increases.

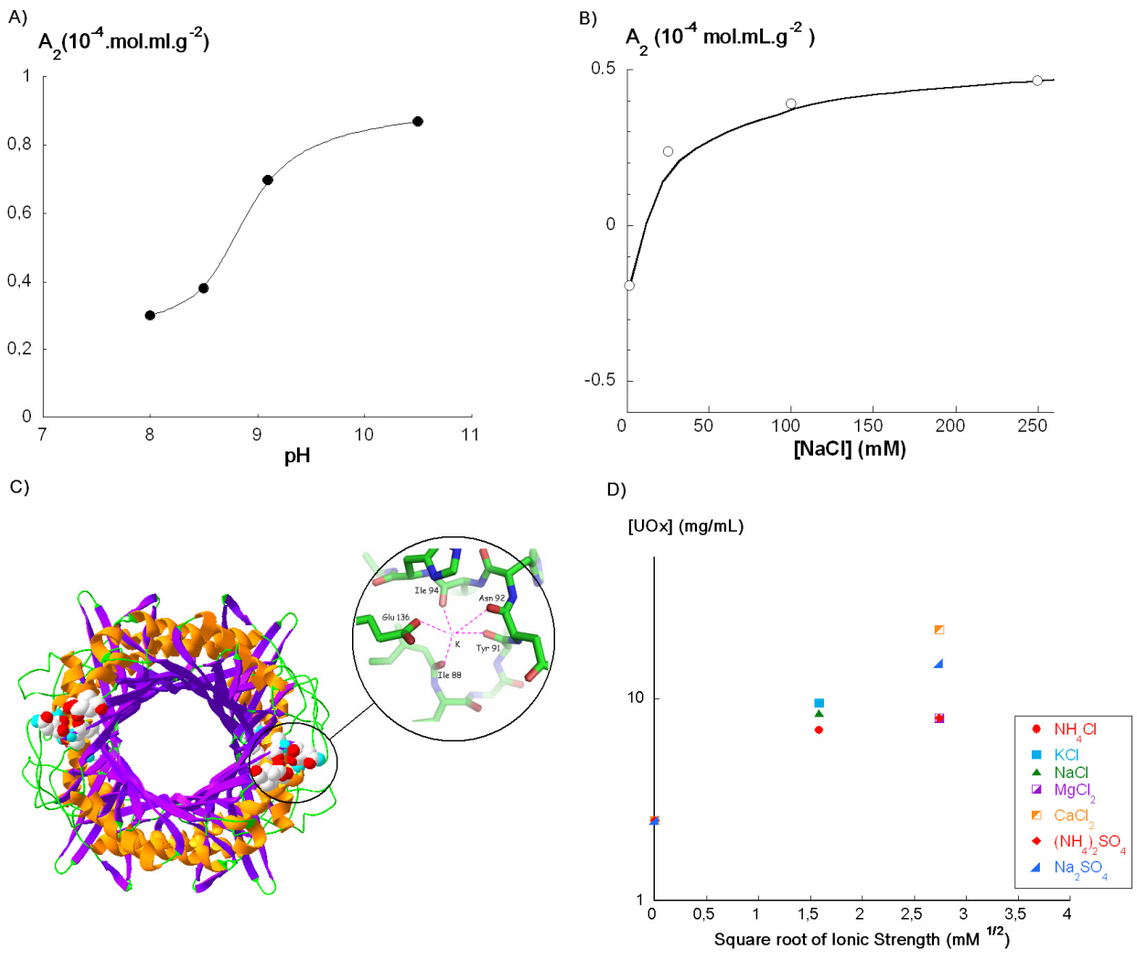


Fig. 8. A) Variation of second virial coefficient ($A_2$) as a function of pH at 20 °C: pH 8.0 with sodium phosphate buffer; pH 9.1 sodium borate buffer; pH 10.5 sodium carbonate buffer. B) Variation of $A_2$ in Tris buffer pH with addition of sodium chloride. C) Cationic binding site on the urate oxidase surface (courtesy of G. Marassio). D) Solubility of urate oxidase as a function of different salt concentrations.

This surprising result suggests that the addition of sodium salt, in particular the addition of sodium cation, induces an increase in repulsion ($A_2 > 0$). Most articles report that addition of salt decreases solubility, which is correlated with the fact that salt induces attractive interactions through charge screening. This effect, known as salting-out (Arakawa & Timasheff, 1985), is generally observed at medium and high salt concentrations. At low ionic strength, the opposite effect is expected, i.e. salting-in, where solubility increases with addition of salt. However, salting-in has only sporadically been reported (Faber et al., 2007). Our result is explained by X-ray crystallography (Fig. 8C), which shows that the salting-in

effect observed with urate oxidase at pH 8 in Tris buffer results from the direct binding of cations to specific sites on the surface of the protein. A similar effect was recently reported (Gibb & Gibb, 2011), which suggests that salting-in is induced by ion binding. This salting-in effect is not specific to sodium cation, since it was observed with different cations such as $K^+$, $NH_4^+$, $Mg^{++}$, $Ca^{++}$ (Fig. 8D). In all cases, the addition of salt induces positive $A_2$ values, an indicator of repulsive interactions with rasburicase, leading to an increase in solubility. Finally, the positive $A_2$ values of urate oxidase in sodium phosphate pH 8 or Tris buffers with 10mM salt are consistent with the high solubility of the protein in these buffers, and the negative $A_2$ value found in tris buffer pH 8 without salt is consistent with attraction inducing crystallization of urate oxidase (Fig. 9A). Obtaining crystals thus made solubility measurements possible (Fig. 9B).

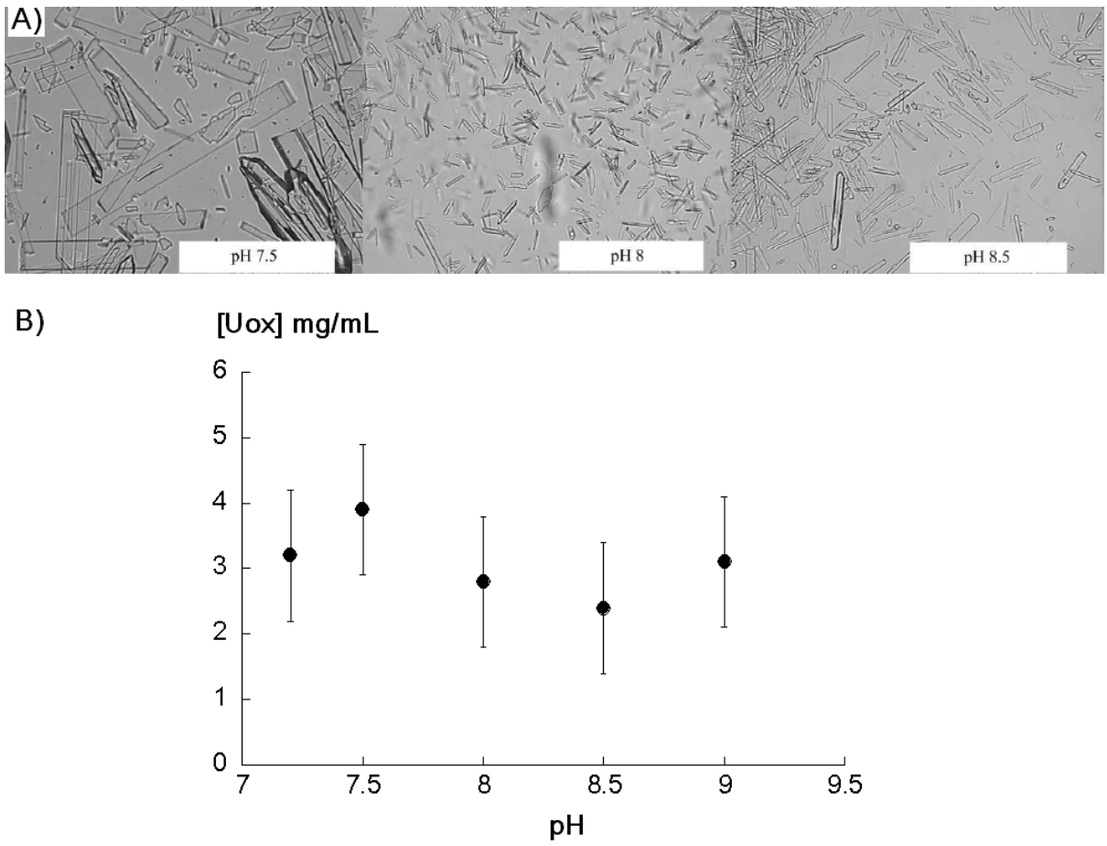


Fig. 9. A) Optical microscopy images of microcrystalline urate oxidase in Tris buffer at different pH values (from Collings et al., 2010). B) Solubility of urate oxidase as a function of pH in Tris buffer w/o salt added.

Even though these crystals were not of sufficient quality for high resolution crystallography, they were perfectly suitable for powder diffraction for space group determination (Collings et al., 2010). Attractive interactions with second virial coefficients in the "crystallization slot" defined by George & Wilson are undoubtedly necessary conditions to obtain crystals; however these interactions must be controlled upstream of the crystallization process to design adequate phase diagrams for appropriate crystallography.

### 4.2 Buffer type and temperature effects

pH and salt effects observed on second virial coefficient variations are easily explained by a change in the coulombic repulsive interactions, either 1/ due to a decrease in the protein net charge, either by shifting pH towards pI or by screening the repulsion with salt at pH far from pI, or 2/ due to an increase in the protein net charge, by ion binding near the pI. The first assumption was verified by characterizing the different underlying interaction potentials (Vivares & Bonneté, 2002) and will not be discussed here. The ion binding effect underlines the importance of choice of solubilization buffer, especially since the objective is to test temperature effect. In previous work, a slight temperature effect was observed on the scattered intensity at small angles at pH 10.5 between 283 and 293 K, and this was attributed to a weak van der Waals attraction. In order to characterize the temperature effect on interaction forces and its implications for crystallization, SAXS experiments were performed over a larger range of temperature from 278 to 303 K at a constant pH closer to the isoelectric point, where the repulsive component is weaker. Since Tris buffer is very sensitive to temperature variations (dpKa/dT = -0.028), we used a borate buffer whose pH is known to be less temperature-dependent (dpKa/dT = -0.008). The scattered intensities of urate oxidase in Tris buffer and in borate buffer at pH 8 as a function of temperature are shown in Fig. 10.

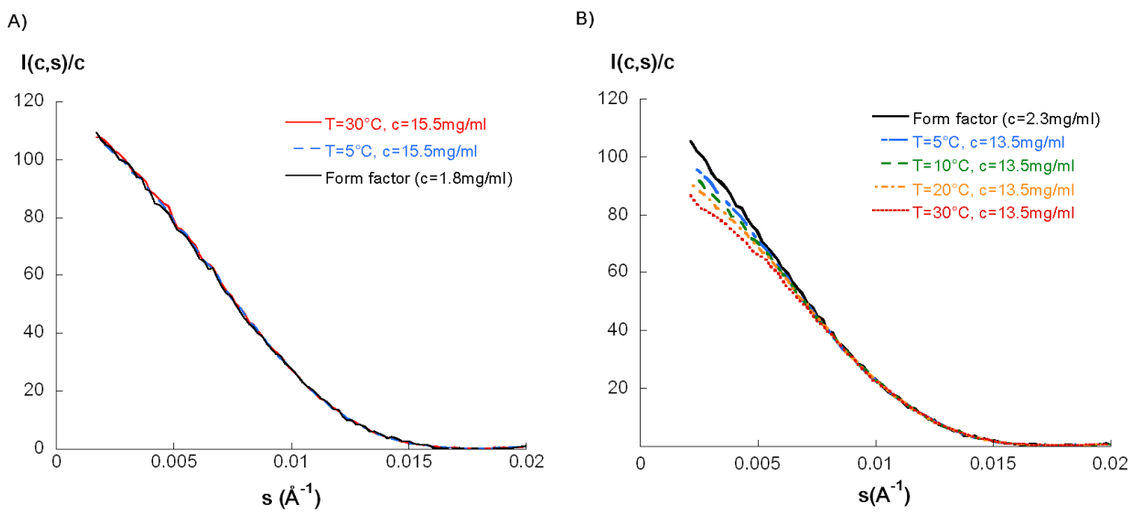


Fig. 10. Variation of scattered intensity of urate oxidase as a function of temperature: A) in tris buffer pH 8; B) in borate buffer pH 8.

It is clear that buffer type influences interactions in urate oxidase in solution. Whereas no variation in intensity is observed in Tris buffer, in borate buffer intensity increases as temperature decreases, probably due to an increase in van der Waals attraction, as previously observed and modelled with lysozyme (Tardieu, et al., 1999).

The second virial coefficient remains positive, probably due to the presence of sodium cations in borate buffer, but decreases as pH decreases (Fig.11A). Since pH in borate buffer does not vary with temperature, the net charge and the repulsive interactions of urate oxidase does not vary. The overall decrease in $A_2$ can only be induced by an increase in attractive interactions, the van der Waals attraction. In contrast, in Tris buffer, pH increases

as the temperature decreases, inducing an increase in the net charge at pH above pI and thus an increase in repulsive interactions, matching the increase in attraction with temperature. This effect can induce the dissolution of crystals obtained at room temperature when stored in cold rooms, for example (data not shown but observed with urate oxidase), even though solubility is direct (Fig. 11B), as in the case of urate oxidase. When care is taken to keep pH constant whatever the temperature, and not to add cations to the buffer, it is therefore possible to obtain crystals and measure solubility (Fig. 11B). Temperature is an important parameter to modify attractive interactions and induce and control crystallization. Nethertheless, the appropriate buffer still needs to be chosen and a significant change in solubility needs to be measured if large crystals are to be grown (Budayova-Spano et al., 2007).

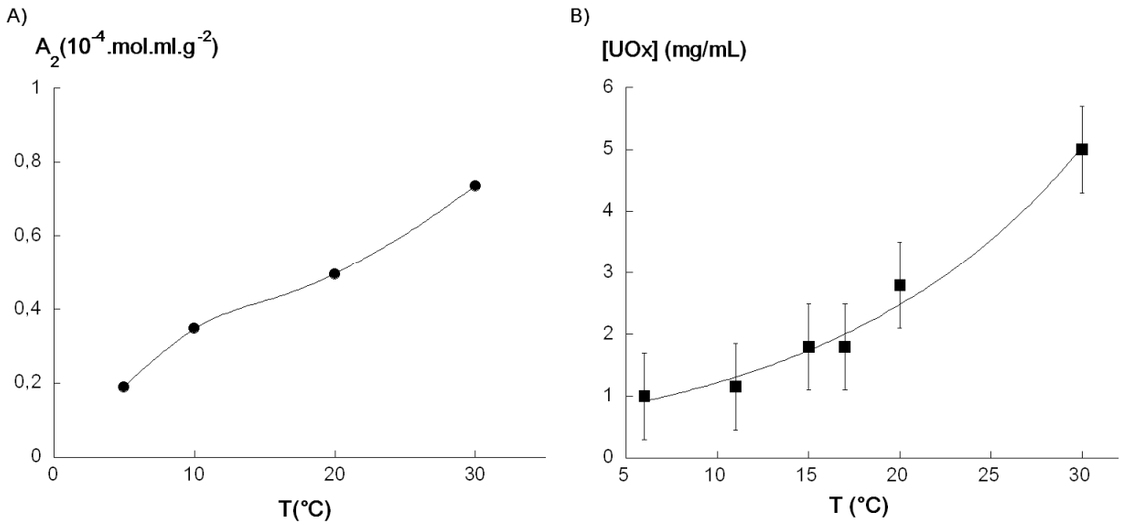


Fig. 11. A) Variation of urate oxidase $A_2$ with temperature in Na borate buffer pH 8; B) Solubility of urate oxidase at pH 8 in tris buffer w/o cations as a function of temperature

### 4.3 Usual and unusual polymers

Salts are known to act as crystallizing agents for many proteins, often small compact proteins, by inducing a short-range attraction. Ions, and in particular anions, were observed, at medium ionic strength, not only to screen charges but to induce an attraction, specific to the salt type (Ducruix, et al., 1996). We have seen here with urate oxidase, a large protein, that specific ion binding can induce solubilization of the protein by inducing a repulsive interaction, preventing its crystallization with salts. When salts are not effective in crystallizing proteins, neutral polymers can do the job (Bonneté et al., 2001; Budayova et al., 1999; Hitscherich, et al., 2000). Polyethylene glycol (PEG), a non-adsorbing neutral polymer, has long been used for protein crystallization (McPherson, 1976). The solubility (actually the precipitation) of proteins in solution containing PEG was studied (Atha & Ingham, 1981). A theoretical model was proposed by Asakura-Oosawa to explain the attraction between colloids due to addition of these polymers (§2.2.3). The effectiveness of polymer in precipitating proteins increases with polymer size and concentration, since it increases the depletion zone. By studying the crystallization of urate oxidase, our group greatly contributed to a better understanding of the mechanism of depletion attraction in the

presence of different polyethylene glycols. We characterized the attractive interactions between urate oxidase induced by addition of three different PEGs (Fig. 12A), obtaining crystals (Fig. 12B) in conditions where $A_2$ was found negative in the "crystallization slot". Compared to salt, a major advantage of PEG in crystallization is that the depth and range of the attraction can be varied almost at will, simply by changing polymer size and concentration. However, it may be appropriate to couple the effects of salts (screening of charges or ion binding) and/or of pH with the effects of polymers to modulate the overall interactions and control the phase diagram for specific design.

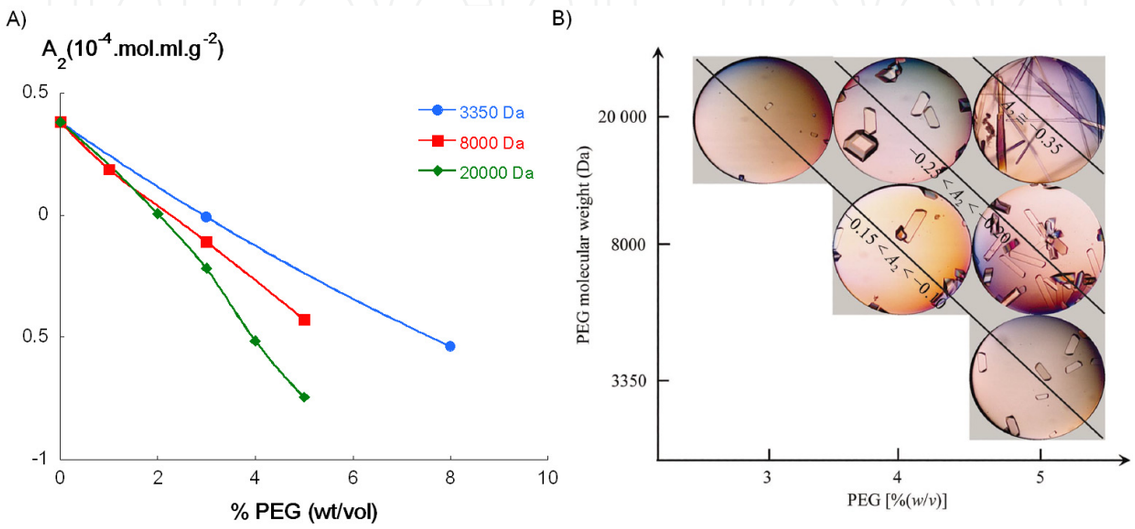


Fig. 12. A) Second virial coefficient urate oxidase in different PEG solutions in Tris pH8. B) Crystals of urate oxidase obtained in attractive ($A_2 < 0$) conditions.

However, as a function of |pH-pI|, the addition of PEG may be insufficient to induce an overall attraction, as shown in figure 13A. Thus, at pH 10, urate oxidase presents repulsive

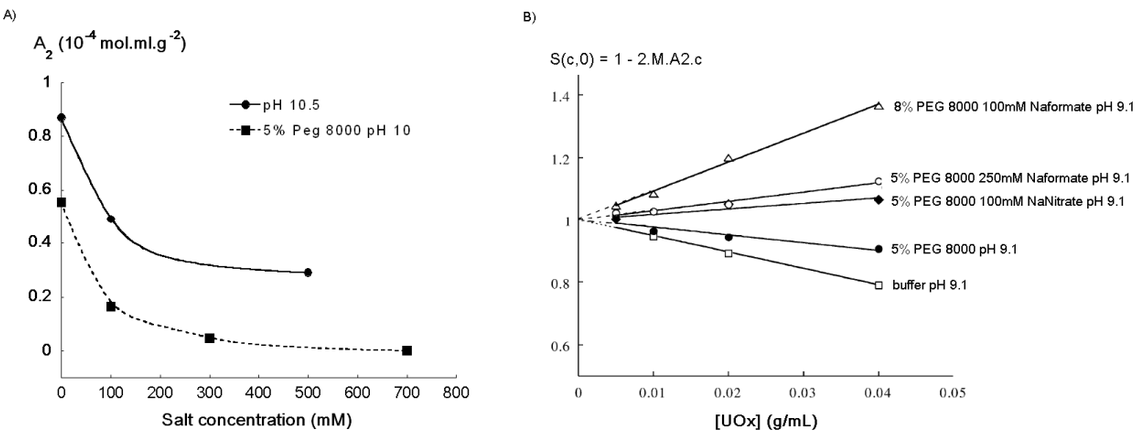


Fig. 13. A) Second virial coefficient of urate oxidase at pH 10 as a function of salt addition far from pI with and w/o PEG. B) Zero-angle structure factor in different physico-chemical conditions as a function of urate oxidase concentration; the slope measures the second virial coefficient (the slope is positive, $A_2$ is negative, attraction and vice versa)

interactions due to the protein negative net charge (see Fig 7). The depletion attraction induced by 5% PEG 8000 is not sufficient to change repulsive interactions into attractive interactions. To induce an overall attraction by addition of PEG, it is necessary to screen charges by addition of salt (Fig13B) or to be close to pI (Fig. 12A), where electrostatic repulsion is lowest.

At pI, regardless of whether salt is present in the buffer (Tris pH8 in our case), the addition of PEG to urate oxidase solutions induces attraction and leads to a decrease in solubility (Fig. 14). However, at pH 8 the solubility of urate oxidase without salt in the buffer is lower than the solubility of urate oxidase with salt. Since nucleation and crystal growth are driven by the supersaturation β, with β the ratio [initial concentration] / [solubility], a limited variation in solubility and therefore in supersaturation will be unfavorable to the growth of large crystals, and will rather favor the nucleation of small crystals.

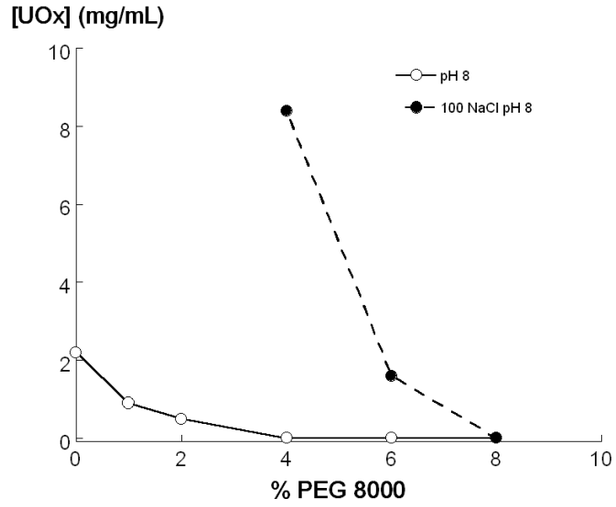


Fig. 14. Solubility of urate oxidase as a function of % of PEG with and w/o salt

As soon as crystals can be obtained, it is therefore possible to characterize the phase diagram with one or several solubility curves depending on the presence of polymorphs and the metastable liquid-liquid phase separation (Fig. 15).

In some cases, salts and neutral polymers are not effective for crystallization or cannot be used in pharmaceutical processes. Other crystallizing agents that can be used include organic compounds such as ethanol (Boyer et al., 1999), isopropanol, methanol, 2-methyl 2,4-pentanediol (Costenaro et al., 2001). Polymers such as amphiphilic multi-block polymers are used in the cosmetic and pharmaceutical industries, more often as emulsifiers, solubilizers, dispersing and wetting agents in the preparation of solid dispersions than as crystallizing agents in biocrystallography or in crystallization processes. We characterized a new class of crystallizing agent for soluble protein crystallization, compatible with both pharmaceutical processes and high-resolution structure determination in bio-crystallography. Poloxamer P188 is a nonionic co-polymer surfactant with a tri-block structure, composed of two hydrophilic segments, poly(oxyethylene) (PEO), and a central hydrophobic segment, poly(oxypropylene) (PPO), linked by ether bonds. The resulting construct can be represented as $HO(C_2H_4O)a(C_3H_6O)b(C_2H_4O)aH$, where a is about 75 and b is about 31 (Takáts et al., 2001) (Fig. 16). Its average molecular weight is around 8400 $g.mol^{-1}$

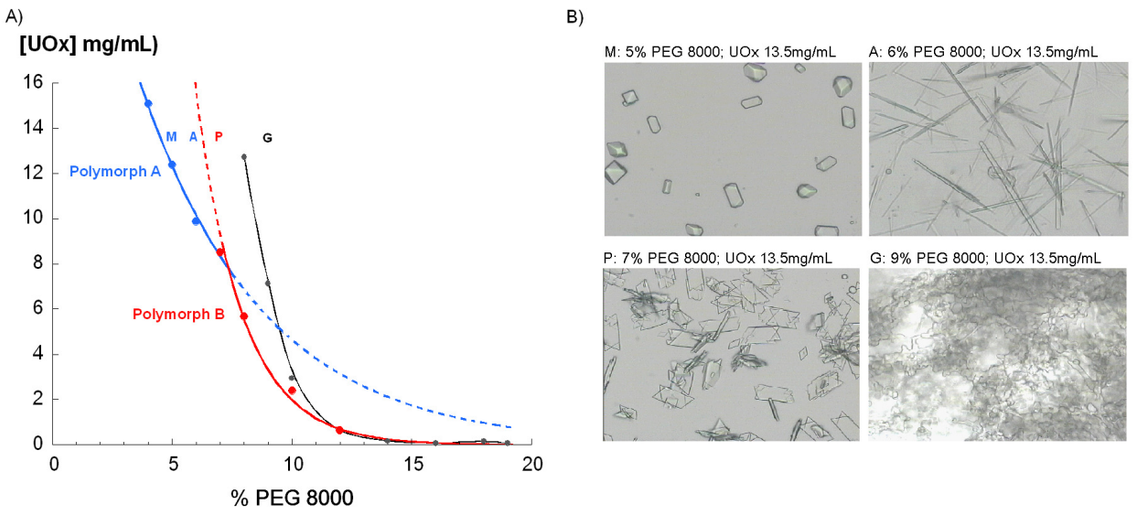


Fig. 15. Phase diagram of urate oxidase in presence of polyethylene glycol 8000 and optical microscopy images of different conditions in this phase diagram (M, A are polymorph A, P polymorph B and G a liquid-liquid phase transition) (Vivares et al., 2006).

and its cmc (critical micellar concentration) is about 0.1 % w/v (Schmolka, 1977). Poloxamer is similar to the usual crystallizing agent for urate oxidase, PEG 8000, which is a linear hydrophilic polymer consisting of approximately n = 180 poly(oxyethylene) units and has a molecular weight of about 8000 $g.mol^{-1}$. Because of their amphiphilic structure, poloxamers have surfactant properties that make them useful in pharmaceutical applications. They can be used to increase water solubility of hydrophobic, oily substances as well as to increase the miscibility of two substances with different hydrophobicities. They are also used as model systems for drug delivery (Adams et al., 2003) applications. Recently, they have been shown to function as artificial chaperones to facilitate refolding of denatured proteins in solution or to suppress aggregation. In general, all these applications require low concentrations of poloxamer, typically below its cmc and involving monomeric poloxamer in solution. Below the cmc, the hydrophobic segment of polymer can non-specifically interact with exposed hydrophobic domains, preventing aggregation and aiding in the refolding of proteins (Lee et al., 2006).

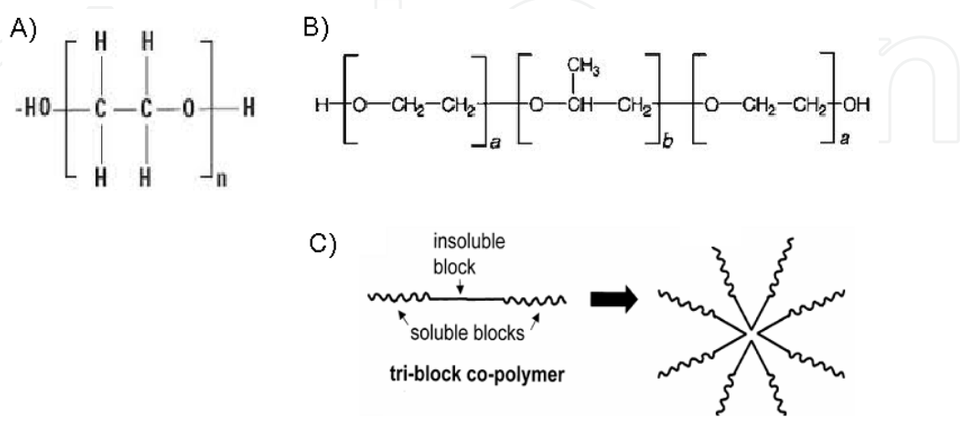


Fig. 16. Chemical structure of poloxamer P188 (A), PEG (B); C) Scheme of micellization of poloxamer at c > cmc (~ 0.1%)

However, high concentrations of poloxamer have also been reported to induce protein aggregation (Garcia, 1975). The addition of 12 to 16 % of the block copolymer to plasma or serum induces the precipitation of high molecular weight proteins including antibodies. This suggests that it would be possible to use high concentrations of poloxamer, thus probably in its micelle form, to induce protein crystallization by depletion, as observed with PEG. To this end, we explored the interactions and crystallization of urate oxidase by addition of poloxamer P188. The second virial coefficient is positive without poloxamer in Tris with 30mM KCl, as expected from previous studies, and increases as the concentration of poloxamer increases up to its cmc (about 0.1%). Above cmc, the $A_2$ decreases and becomes negative at concentrations higher than 1%. Solubility of urate oxidase was therefore measured in the same conditions, as a function of concentration of poloxamer P188. As with PEG 8000, solubility decreases as the concentration of poloxamer increases and is higher with poloxamer P188 than with PEG 8000 for concentrations lower than 6 % (Fig. 17). Thus, the surfacting or crystallizing nature of poloxamer P188 depends on its concentration. Below 0.1 %, i.e. its cmc, poloxamer is monomeric. In this range of concentrations, it is possible that the hydrophobic central PPO block non-specifically interacts with solvent-exposed hydrophobic patches at the protein's surface, while the hydrophilic surfactant chains remain exposed to the aqueous phase, increasing the solubility and the repulsion of urate oxidase. Above 0.1 % poloxamer, micelles can form. The attractive effect of poloxamer at concentrations above 1 % can be explained by a depletion effect driven by poloxamer micelles. The same effect has been suggested with nanoemulsions whose micelles, after surface saturation by surfactant, do not adsorb on the surface but rather cause attraction by a depletion mechanism (Wulff-Pérez et al., 2009).

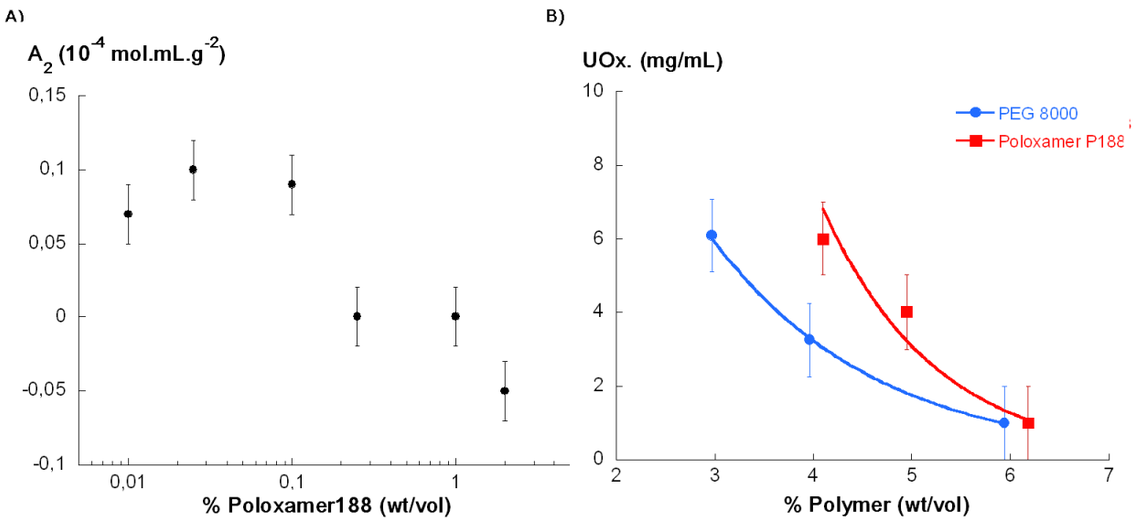


Fig. 17. A) Second virial coefficient of urate oxidase in solution as a function of % Poloxamer P188. B) Comparison between solubility of urate oxidase in PEG 8000 and Poloxamer P188 in 30 mM KCl, 50 mM Tris pH 7.5 at 20°C.

Poloxamer P188 can thus be used as a crystallizing agent for urate oxidase. When other amphiphilic surfactants such as poloxamer P407, polysorbate 20 and polysorbate 80 were studied, poloxamer P407 was found to have a similar structure and molecular formula to poloxamer P188, where a and b are 100 and 60 respectively. The molecular weight of the

hydrophobic core is 4000 g.mol-1, which represents 30 % of the total mass of the polymer. P407 average molecular weight is about 13300 g.mol$^{-1}$. As shown in Fig. 18A, urate oxidase solubility in poloxamer P407 is higher than in either poloxamer P188 or PEG 8000, when the remaining solution components are kept fixed (i.e. 50 mM Tris pH 7.5, 30 mM KCl). Unlike PEG, urate oxidase solubility increases with the mass of the poloxamer used. This result suggests that poloxamer has a solubilizing effect proportional to its hydrophobic core content, and this compensates for its precipitating by depletion. The effect of polysorbates, another class of emulsifiers used in the preparation of pharmaceuticals and food, was also tested. Polysorbates are oily liquids derived from PEGylated sorbitan (a sorbitol derivative) esterified with fatty acids. They all have a hydrophilic moiety characterized by twenty oxyethylene-($CH_2CH_2O$)- groups, while the hydrophobic segments vary according to the polysorbate compound. Polysorbates 20 and 80 effectively induce crystallization of urate oxidase (Fig. 18B). Urate oxidase solubility is higher with polysorbates 20 and 80 than with PEG 8000 and poloxamers P188 and P407. As with poloxamers, it appears that the longer the polysorbate hydrophobic chain, the higher the solubility of urate oxidase. Nevertheless, the modification observed in the habit of the urate oxidase crystals with 16% polysorbate 80 suggests that this concentration of surfactant could affect crystal growth, and possibly protein structure.

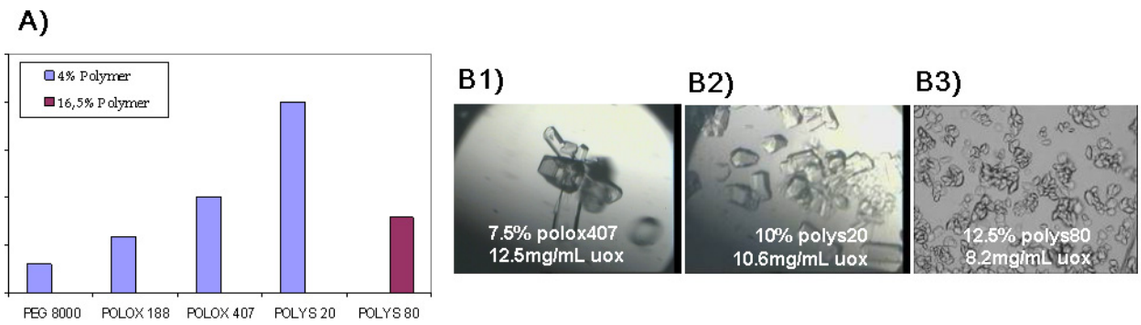


Fig. 18. A) Urate oxidase solubility with various polymers (in 30 mM KCl, 50 mM Tris pH7.5, 20°C). B) Crystals of urate oxidase in 30 mM KCl, 50 mM Tris pH7.5, 20°C: B1) 12.5 mg.mL$^{-1}$ uox with 7.5 % poloxamer P407; B2) 10.6 mg.mL$^{-1}$ uox with 10 % polysorbate 20; B3) 8.2 mg.mL$^{-1}$ uox with 12.5 % polysorbate 80.

### 4.4 Urate oxidase crystal design for high pressure crystallography

Macromolecules were long supposed to have their own crystallization conditions, since they have a unique sequence. However, the fact is that macromolecules in solution interact through different weak interaction forces. They can be considered as charged colloids under the influence of attraction forces (van der Waals, depletion, Hofmeister) and repulsion forces (hard sphere, electrostatic). These forces are medium-range and each of them is under the separate control of physico-chemical conditions such as pH, temperature and solvent composition. These forces govern macromolecule properties in solution such as solubility, phase separation (liquid-liquid or liquid-solid). The fine tuning of these interaction forces makes the design of phase diagrams for specific applications possible. The overall attractive potential leading to crystallization can be obtained in different ways. We used urate oxidase as a model system, since it was available in large quantities, to explore a wide spectrum of physico-chemical conditions and to see how these parameters influence pair potentials and

phase diagrams. For example, the salting-in effect by increasing repulsion allows us to modulate the position of the solubility curve in the urate oxidase phase diagram, leading to a more or less large metastable zone, in order to grow either large single crystals or numerous small crystals. Another example is the use of amphiphilic polymer below or above its cmc (critical micellar concentration), allowing us either to favor the solubility of proteins or to induce their crystallization. In the following example, we describe a strategy for growing protein crystals suitable for macromolecular crystallography under high pressure (HPMX). Studying proteins under high pressure encompasses a wide range of objectives, from understanding the physical chemistry of protein interactions with water to practical applications in food processing. Many proteins are studied using a variety of techniques applied under high pressure, such as spectroscopic techniques, NMR spectroscopy, as well as a wide range of scattering techniques including static and dynamic light scattering, neutron scattering and X-ray crystallography. Such high-pressure approaches are generally used to solve problems involving macromolecule structural changes. For High Pressure Macromolecular Crystallography (HPMX), obtaining the right protein crystal is a challenge. First, as for any crystallographic study, it is necessary to obtain a reasonably large crystal preferentially in a high symmetry space group. Secondly, the crystal has to fit the pressure cell as well as possible, and be grown by a method which allows the crystal to be picked out easily, for example the hanging drop technique. Finally, the crystal has to remain stable in its mother liquor under pressure. Indeed, the effect of pressure on protein nucleation and crystallization can vary widely. In some cases, increased pressure increases the nucleation rate (Visuri et al., 1990), while in other cases, the protein solubility increases, decreasing the nucleation rate (Lorber et al., 1996). Pressure can affect solubility and therefore lead either to dissolution of a crystal or to secondary nucleation. To circumvent the pressure effect on secondary crystal nucleation in the cell, the crystal must be placed in a mother liquor containing no protein and a high concentration of crystallizing agent, since variations in solubility caused by pressure are known to be reduced by increasing the crystallizing agent concentration.

To grow a suitable crystal for HPMX, we first need a low supersaturation $\beta$ which will lead to a small number of large crystals rather than a large number of small crystals, finally yielding a crystal in equilibrium with a very low protein solution, i.e. at high crystallizing agent concentration. To optimize urate oxidase crystallization conditions, we first characterize the phase diagram without salt, i.e. the conditions where solubility is lowest, as a function of PEG percentage (Fig. 19A) and explore different crystal growth conditions by using the Microbatch technique (Chayen et al., 1992).

The rasburicase crystals obtained as a function of PEG 8000 are of two different shapes: tabular crystals when the percentage of PEG is below 4%, and plate-like crystals when PEG percentage is above 4% (Fig. 19B). Unfortunately, crystals obtained at the lowest solubility, i.e. when percentages of PEG are greatest, are not suitable for crystal diffraction studies, being too numerous and poorly faceted. A suitable tabular crystal grown at a lower PEG percentage is picked out and placed in a glass cell. According to the solubility curve in 50mM Tris pH8, rasburicase is totally insoluble in a solution of more than 10% PEG 8000. To control the stability of the crystal, protein-free mother liquor (15% PEG 8000, 50mM tris pH 8.0) is added to the crystal. The solubility, i.e. the concentration of the protein solution $\Delta c$ remaining around the picked-out crystal, being too high, this leads to a secondary nucleation around the crystal (Fig. 19C). Indeed, the remaining protein solution around the crystal diluted in the protein-free mother liquor is supersatured and induces a new

nucleation. The crystallization conditions must therefore be a compromise between solubility which is sufficient to grow large crystals but not too high, so as to avoid secondary nucleation when the mother liquor is added.

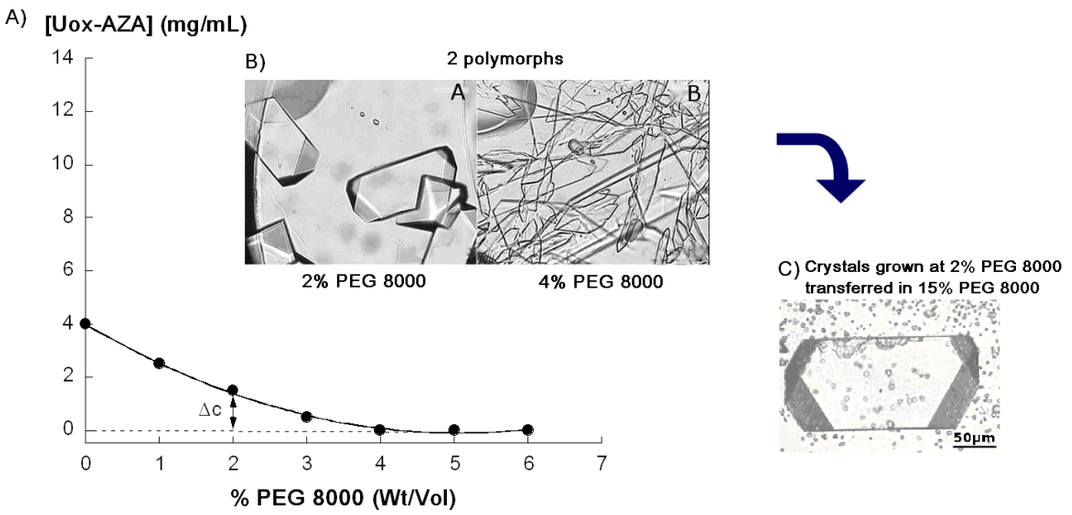


Fig. 19. A) Solubility of urate oxidase complexed with 8-azaxanthine, in Tris buffer pH 8, without salt, as a function of PEG 8000; B) Micrographs of urate oxidase crystals grown in microbatch at two PEG percentages; C) Micrograph of urate oxidase crystals transferred in 15% PEG 8000.

Therefore, to obtain a massive-habit crystal at high PEG percentage, we added 100mM NaCl, despite the salting-in effect which increases solubility, and determined the new solubility curve as a function of PEG 8000 (Fig. 20A).

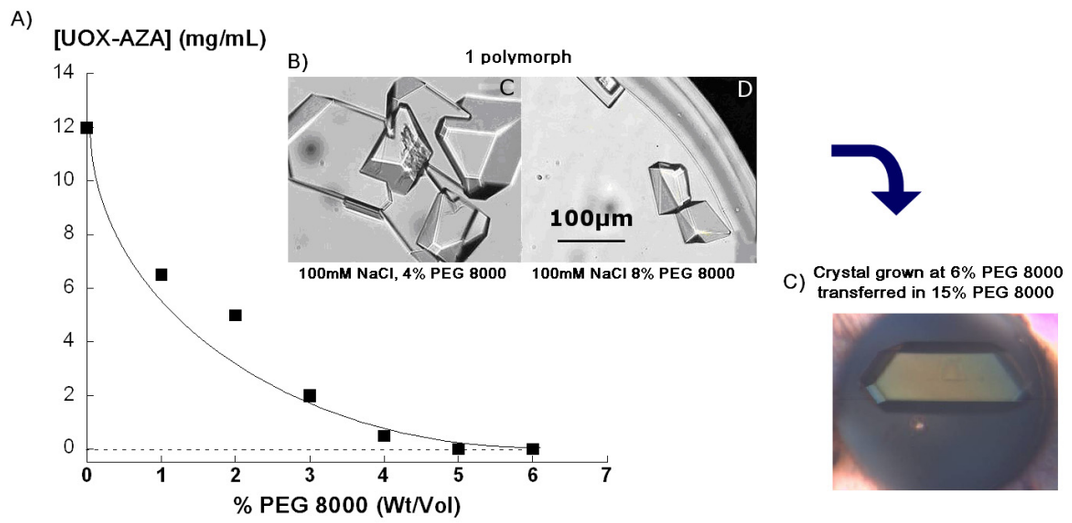


Fig. 20. A) Solubility of urate oxidase complexed with 8-azaxanthine, in Tris buffer pH 8, with 100mM NaCl, as a function of PEG 8000; B) Micrographs of urate oxidase crystals grown in microbatch at two PEG percentages; C) Micrograph of urate oxidase crystal transferred in 15% PEG 8000.

Crystal habits become more suitable for crystal diffraction studies (Fig. 20B) with sizes compatible with the pressure cell dimensions. We successfully transfer a crystal grown in 3.2mg/mL of urate oxidase 6% PEG 100mM NaCl Tris 50mM pH8 into a solution of 15% PEG 8000, 100mM NaCl, 50mM tris pH 8.0. It remains stable for more than one week without secondary nucleation appearing (Fig. 20C). At this concentration of protein, no micro-crystals are generated from the solution surrounding the crystal, whereas at lower PEG and higher protein concentrations in the surrounding solution, many micro-crystals grow.

## 5. Conclusion

Distribution of macromolecules in solution, phase diagrams and the crystallization process are governed by an appropriate combination of interaction potentials in solution. Three types of parameters or additives appear to play a crucial role: pH, salt and polymers. Whatever the diversity of protein sequences, it is possible, via second virial coefficient measurements, to limit the number of trials for a first screening of crystallization conditions and to rationalize crystallization. The design of small crystals or large diffracting crystals then results from a subtle mix of strong or weak repulsions and attractions, which control the position of the solubility curve and the metastable zone in the phase diagram.

## 6. Acknowledgment

This work was carried out by Denis Vivarès (1998-2003) and Marion Giffard (2006-2009) during their PhD theses. We gratefully acknowledge the generous support of Bertrand Castro, Mohamed El Hajji and François Ragot from Sanofi-Aventis (France) for this project on fundamental crystallization of urate oxidase since 1998, and their subsequent PhD financial support (2006-2009) enabling us to study the crystallization of urate oxidase for industrial applications.

## 7. References

Adams, M. L.; Lavasanifar, A. & Kwon, G. S. (2003). Amphiphilic block copolymers for drug delivery. *Journal of Pharmaceutical Sciences*, Vol. 92, No. 7, pp. 1343-1355,

Aleman, C.; Bayol, A.; Breul, T. & Dupin, P. (1998). Stable liquid composition containing urate oxidase and lyophilized composition for its preparation. Sanofi, Paris. United States

Arakawa, T. & Timasheff, S. (1985). Theory of protein solubility. *Methods in Enzymology*, Vol. 114, No. pp. 49-77, ISSN: 0076-6879

Asakura, S. & Oosawa, F. (1954). On the interaction between two bodies immersed in a solution of macromolecules. *J. Chem. Phys.*, Vol. 22, No. pp. 1255-1256,

Asherie, N.; Lomakin, A. & Benedek, G. B. (1996). Phase diagram of colloidal solutions. *Physical Review Letters*, Vol. 77, No. 23, pp. 4832-4835, ISSN: 0031-9007

Atha, D. H. & Ingham, K. C. (1981). Mechanism of precipitation of proteins by polyethylene glycols. Analysis in terms of excluded volume. *The Journal of biological chemistry*, Vol. 256, No. 23, pp. ISSN: 0021-9258

Bayol, A.; Dupin, P.; Boe, J. F.; Claudy, P. & Létoffé, J. M. (1995). Study of pH and temperature-induced transitions in urate oxidase (Uox-EC1.7.3.3) by microcalorimetry (DSC), size exclusion chromatography (SEC) and enzymatic activity experiments. *Biophysical Chemistry*, Vol. 54, No. 3, pp. 229-235, ISSN: 0301-4622

Behlke, J. & Ristau, O. (1999). Analysis of the thermodynamic non-ideality of proteins by sedimentation equilibrium experiments. *Biophysical Chemistry*, Vol. 76, No. 1, pp. 13-23, ISBN 0301-4622

Belloni, L. (1985). A hypernetted chain study of highly asymmetrical polyelectrolytes. *Chemical Physics*, Vol. 99, No. 1, pp. 43-54,

Belloni, L. (1988). Self-consistent integral equation applied to the highly charged primitive model. *J. Chem. Phys.*, Vol. 88, No. 8, pp. 5143-5148,

Belloni, L. (1991). Interacting monodisperse and polydisperse spheres, In: *Neutron, X-ray and light scattering*, Series, N.-H.D., pp. 135-155, Elsevier Science Publishers B.V., Amsterdam-Oxford-NewYork-Tokyo

Bergfors, T. (2009). Protein Crystallization ISBN-13: 978-0972077446,

Bhamidi, V.; Varanasi, S. & Schall, C. A. (2005). Protein Crystal Nucleation: Is the Pair Interaction Potential the Primary Determinant of Kinetics? *Langmuir*, Vol. 21, No. 20, pp. 9044-9050, ISBN 0743-7463

Bloustine, J.; Berejnov, V. & Fraden, S. (2003). Measurements of Protein-Protein Interactions by Size Exclusion Chromatography. *Biophysical Journal*, Vol. 85, No. 4, pp. 2619-2623, ISSN: 0006-3495

Bolhuis, P. G.; Louis, A. A.; Hansen, J. P. & Meijer, E. J. (2001). Accurate effective pair potential for polymer solutions. *J.Chem.Phys.*, Vol. 114, No. 9, pp. 4296-4311,

Bonneté, F. & Vivares, D. (2002). Interest of the normalized second virial coefficient and interaction potentials for crystallizing large macromolecules. *Acta Cryst*, Vol. D58, No. pp. 1571-1575, ISSN: 0907-4449

Bonneté, F.; Finet, S. & Tardieu, A. (1999). Second virial coefficient: variations with lysozyme crystallization conditions. *J. Crystal Growth*, Vol. 196, No. pp. 403-414, ISSN: 0022-0248

Bonneté, F.; Vivares, D.; Robert, C. & Colloc'h, N. (2001). Interactions in solution and crystallization of *Aspergillus flavus* urate oxidase. *J. Crystal Growth*, Vol. 232, No. pp. 330-339, ISSN: 0022-0248

Boué, F.; Lefaucheux, F.; Robert, M. C. & Rosenman, I. (1993). Small angle neutron scattering study of lysozyme solutions. *Journal of Crystal Growth*, Vol. 133, No. 3-4, pp. 246-254, ISBN 0022-0248

Boyer, M.; Roy, M.-O.; Jullien, M.; Bonnete, F. & Tardieu, A. (1999). Protein interactions in concentrated ribonuclease solutions. *J. Crystal Growth*, Vol. 196, No. 2-4, pp. 185-192,

Budayova, M.; Bonneté, F.; Tardieu, A. & Vachette, P. (1999). Interactions in solution of large oligomeric protein. *J. Crystal Growth*, Vol. 196, No. pp. 210-219, ISSN: 0022-0248

Budayova-Spano, M.; Dauvergne, F.; Audiffren, M.; Bactivelane, T. & Cusack, S. (2007). A methodology and an instrument for the temperature-controlled optimization of crystal growth. *Acta Crystallographica Section D-Biological Crystallography*, Vol. 63, No. pp. 339-347, ISSN: 0907-4449

Carbonnaux, C.; Riès-Kautt, M. & Ducruix, A. (1995). Relative effectiveness of various anions on the solubility of acidic Hypoderma lineatum collagenase at pH 7.2. *Protein Science*, Vol. 4, No. 10, pp. 2123-2128, ISSN: 0961-8368

Casselyn, M.; Perez, J.; Tardieu, A.; Vachette, P.; Witz, J. & Delacroix, H. (2001). Spherical plant viruses: interactions in solution, phase diagrams and crystallization of brome mosaic virus. *Acta Crystallographica Section D-Biological Crystallography*, Vol. 57, No. pp. 1799-1812, ISSN: 0907-4449

Chayen, N. E.; Stewart, P. D. S. & Blow, D. M. (1992). Microbatch Crystallization under Oil - a New Technique Allowing Many Small-Volume Crystallization Trials. *Journal of Crystal Growth*, Vol. 122, No. 1-4, pp. 176-180, ISSN: 0022-0248

Chernov, A. A. (2003). Protein crystals and their growth. *Journal of Structural Biology, Macromolecular crystallization in the structural genomics era*, Vol. 142, No. 1, pp. 3-21, ISSN: 1047-8477

Collings, I.; Watier, Y.; Giffard, M.; Dagogo, S.; Kahn, R.; Bonnete, F.; Wright, J. P.; Fitch, A. N. & Margiolaki, I. (2010). Polymorphism of microcrystalline urate oxidase from Aspergillus flavus. *Acta Crystallographica Section D-Biological Crystallography*, Vol. 66, No. pp. 539-548, ISSN: 0907-4449

Costenaro, L.; Zaccai, G. & Ebel, C. (2001). Understanding the crystallisation of an acidic protein by dilution in the ternary NaCl-2-methyl-2,4-pentanediol-H2O system. *J. Crystal Growth*, Vol. 232, No. pp. 102-113,

Debye, P. (1946). The Intrinsic Viscosity of Polymer Solutions. *J.Chem.Phys.*, Vol. 14, No. pp. 636-646,

Drenth, J. (2005). The nucleation of lysozyme from a fluctuation point of view. *Crystal Growth & Design*, Vol. 5, No. 3, pp. 1125-1127, ISSN: 1528-7483

Ducruix, A.; Guilloteau, J. P.; Riès-Kautt, M. & Tardieu, A. (1996). Protein interactions as seen by solution X-ray scattering prior to crystallogenesis. *J. Crystal Growth*, Vol. 168, No. pp. 28-39, ISSN 0022-0248

Faber, C.; Hobley, T.; Mollerup, J.; Thomas, O. R. T. & Kaasgaard, S. (2007). Study of the Solubility of a Modified Bacillus licheniformis r-Amylase around the Isoelectric Point. *Journal of Chemical and Engineering Data*, Vol. 52, No. pp. 707-713, ISSN: 0021-9568

Feher, G. & Kam, Z. (1985). Nucleation and growth of protein crystals: general principles and assays. *Method Enzymol.*, Vol. 114, No. pp. 77–112, ISSN: 00766879

Finet, S. & Tardieu, A. (2001). alpha-cristallin interaction forces studied by small angle X-ray scattering and numerical simulations. *J. Crystal Growth*, Vol. 232, No. 1-4, pp. 40-49, ISSN: 0022-0248

Finet, S.; Bonneté, F.; Frouin, J.; Provost, K. & Tardieu, A. (1998). Lysozyme crystal growth, as observed by small angle X-ray scattering, proceeds without crystallization intermediates. *European Biophysics Journal*, Vol. 27, No. 3, pp. 263-271, ISBN 0175-7571

Finet, S.; Skouri-Panet, F.; Casselyn, M.; Bonneté, F. & Tardieu, A. (2004). The Hofmeister effect as seen by SAXS in protein solutions. *Current Opinion in Colloid & Interface Science*, Vol. 9, No. 1-2, pp. 112-116, ISSN: 1359-0294

Garcia, L. A. (1975). Production of antisera comprising fractionating plasma or serum with an ethylene oxide-polyoxypropylene block copolymer. Baxter Laboratories, Inc. United States of America

García-Ruiz, J.-M. (2003). Nucleation of protein crystals. *Journal of Structural Biology, Macromolecular crystallization in the structural genomics era*, Vol. 142, No. 1, pp. 22-31, ISSN: 1047-8477

Gavira, J. A. & Garcia-Ruiz, J. M. (2009). Effects of a Magnetic Field on Lysozyme Crystal Nucleation and Growth in a Diffusive Environment. *Crystal Growth & Design*, Vol. 9, No. 6, pp. 2610-2615, ISSN: 1528-7483

George, A. & Wilson, W. W. (1994). Predicting protein crystallization from a dilute solution property. *Acta Crystallographica*, Vol. D50, No. 4, pp. 361-365, ISSN: 0907-4449

Gibb, C. L. D. & Gibb, B. C. (2011). Anion Binding to Hydrophobic Concavity Is Central to the Salting-in Effects of Hofmeister Chaotropes. *Journal of the American Chemical Society J. Am. Chem. Soc.*, Vol. 133, No. 19, pp. 7344-7347, ISSN: 0002-7863

Giffard, M.; Colloc'h, N.; Ferté, N.; Castro, C. & Bonneté, F. (2008). Salting-in effect on urate oxidase crystal design. *Crystal Growth and Design*, Vol. 8, No. pp. 4220-4226, ISSN: 1932-6203

Giffard, M.; Ferté, N.; Ragot, F.; El Hajji, M.; Castro, B. & Bonneté, F. (2011). Urate Oxidase Purification by Salting-in Crystallization: Towards an Alternative to Chromatography. *Plos One*, Vol. 6, No. 5, pp. WOS:000290483600005

Gripon, C.; Legrand, L.; Rosenman, I.; Vidal, O.; Robert, M. C. & Boué, F. (1997). Lysozyme-lysozyme interactions in under- and super-saturated solutions: a simple relation between the second virial coefficients in H2O and D2O. *Journal of Crystal Growth*, Vol. 178, No. 4, pp. 575-584, ISBN 0022-0248

Guilloteau, J.-P.; Rie`s-Kautt, M. M. & Ducruix, A. F. (1992). Variation of lysozyme solubility as a function of temperature in the presence of organic and inorganic salts. *Journal of Crystal Growth*, Vol. 122, No. 1-4, pp. 223-230, ISSN: 0022-0248

Guinier, A. & Fournet, G. (1955). Small angle scattering of X-rays Wiley, New York

Hansen, J. P. & McDonald, I. R. (1976). Theory of simple liquids Academic Press, London - New York - San Francisco

Haynes, C. A.; Tamura, K.; Korfer, H. R.; Blanch, H. W. & Prausnitz, J. M. (1992). Thermodynamic properties of aqueous .alpha.-chymotrypsin solution from membrane osmometry measurements. *The Journal of Physical Chemistry*, Vol. 96, No. 2, pp. 905-912, ISSN: 0022-3654

Hitscherich, C. J.; Kaplan, J.; Allaman, M.; Wiencek, J. & Loll, P. J. (2000). Static light scattering studies of OmpF porin : implications for integral membrane protein crystallization. *Protein Sci.*, Vol. 9, No. pp. 1559-1566, ISSN: 0961-8368

Israelachvili, J. (1994). Intermolecular and surface forces New York

Jacobsen, C.; Garside, J. & Hoare, M. (1998). Nucleation and growth of microbial lipase crystals from clarified concentrated fermentation broths. *Biotechnology and Bioengineering*, Vol. 57, No. 6, pp. 666-675, ISSN: 0006-3592

Lee, R. C.; Despa, F.; Guo, L.; Betala, P.; Kuo, A. & Thiyagarajan, P. (2006). Surfactant copolymers prevent aggregation of heat denatured lysozyme. *Annals of Biomedical Engineering*, Vol. 34, No. 7, pp. 1190-1200, ISI:000239085800012

Lekkerkerker, H. N. W. (1997). Strong, weak and metastable liquids. *Physica A*, Vol. 244, No. pp. 227-237, ISSN: 0378-4371

Liu, Y. X.; Wang, X. J. & Ching, C. B. (2010). Toward Further Understanding of Lysozyme Crystallization: Phase Diagram, Protein-Protein Interaction, Nucleation Kinetics, and Growth Kinetics. *Crystal Growth & Design*, Vol. 10, No. 2, pp. 548-558, ISSN: 1528-7483

Lomakin, A.; Asherie, N. & Benedek, G. B. (1996). Monte Carlo study of phase separation in aqueous protein solutions. *Journal of Chemical Physics*, Vol. 104, No. 4, pp. 1646-1656, ISSN: 0021-9606

Lorber, B.; Jenner, G. & Giégé, R. (1996). Effect of high hydrostatic pressure on nucleation and growth of protein crystals. *J. Crystal Growth*, Vol. 158, No. 1-2, pp. 103-117, ISSN: 0022-0248

Lovgren, S. (2007). Giant Crystal Cave's Mystery Solved. *National Geographic News*

Lutterbach, N.; Versmold, H.; Reus, V.; Belloni, L. & Zemb, T. (1999a). Charge-stabilized liquidlike ordered binary colloidal suspensions. 1. Ultra-Small-Angle X-ray Scattering characterization. *Langmuir*, Vol. 15, No. pp. 337-344, ISSN: 0743-7463

Lutterbach, N.; Versmold, H.; Reus, V.; Belloni, L.; Zemb, T. & Lindner, P. (1999b). Charge-stabilized liquidlike ordered binary colloidal suspensions. 2. Partial structure factors determined by Small-Angle Neutron Scattering. *Langmuir*, Vol. 15, No. pp. 345-352, ISSN: 0743-7463

Malfois, M.; Bonneté, F.; Belloni, L. & Tardieu, A. (1996). A model of attractive interactions to account for liquid-liquid phase separation of protein solutions. *J. Chem. Phys.*, Vol. 105, No. B, pp. 3290-3300, ISSN: 0021-9606

McGrath, B. & Walsh, G. (2005). Directory of Therapeutic Enzymes CRC Press Inc, ISBN-10: 0849327148,

McPherson, A. (1976). Crystallization of proteins from polyethylene glycol. *The Journal of biological chemistry*, Vol. 251, No. 20, pp. 6300-6303, ISSN: 0021-9258

McPherson, A.; Malkin, J. A.; Kuznetsov, Y. G.; Koszelak, S.; Wells, M.; Jenkins, G.; Howard, J. & Lawson, G. (1999). The effects of microgravity on protein crystallization: evidence for concentration gradients around growing crystals. *Journal of Crystal Growth*, Vol. 196, No. 2-4, pp. 572-586, IBSN 0022-0248

McQuarrie, D. A. (2000). Statistical mechanics Sausalito, CA

Mikol, V.; Hirsch, E. & Giegé, R. (1989). Monitoring protein crystallization by dynamic light scattering. *FEBS Letters*, Vol. 258, No. 1, pp. 63-66, ISBN 0014-5793

Muschol, M. & Rosenberger, F. (1995). Interactions in under- and supersaturated lysozyme solutions. Static and dynamic light scattering results. *J. Chem. Phys.*, Vol. 103, No. 24, pp. 10424-10432, ISSN: 0021-9606

Ng, J. D.; Gavira, J. A. & García-Ruíz, J. M. (2003). Protein crystallization by capillary counterdiffusion for applied crystallographic structure determination. *Journal of Structural Biology, Macromolecular crystallization in the structural genomics era*, Vol. 142, No. 1, pp. 218-231, ISBN 1047-8477

Oksanen, E.; Blakeley, M. P.; Bonnete, F.; Dauvergne, M. T.; Dauvergne, F. & Budayova-Spano, M. (2009). Large crystal growth by thermal control allows combined X-ray and neutron crystallographic studies to elucidate the protonation states in Aspergillus flavus urate oxidase. *Journal of the Royal Society Interface*, Vol. 6, No. pp. S599-S610, ISSN: 1742-5689

Pande, A.; Pande, J.; Asherie, N.; Lomakin, A.; Ogun, O.; King, J. & Benedek, G. B. (2001). Crystal cataracts: human genetic cataract caused by protein crystallization. *PNAS*, Vol. 98, No. 11, pp. 6116-6120, ISBN 0027-8424

Poon, W. C. K. (2002). The physics of a model colloid-polymer mixture. *Journal of Physics-Condensed Matter*, Vol. 14, No. 33, pp. R859-R880, ISSN: 0953-8984

Retailleau, P.; Colloc'h, N.; Vivares, D.; Bonneté, F.; Castro, B.; El Hajji, M.; Mornon, J. P.; Monard, G. & Prangé, T. (2004). Complexed and ligand-free high resolution structures of Urate oxidase (Uox) from *Aspergillus flavus*: a re-assignation of the active site binding mode. *Acta Cryst*, Vol. D60, No. pp. 453-462, ISSN: 0907-4449

Retailleau, P.; Colloc'h, N.; Vivares, D.; Bonneté, F.; Castro, B.; El Hajji, M. & Prangé, T. (2005). Urate oxidase from Aspergillus flavus: new crystal-packing contacts in relation to the content of the active site. *Acta Cryst.*, Vol. D61, No. pp. 218-229, ISSN: 0907-4449

Riès-Kautt, M. & Ducruix, A. (1999). From solution to crystals with a physico-chemical aspect, In: *Crystallization of nucleic acids and proteins - A practical approach,* Giegé, R., pp., Oxford University Press, Oxford, New York, Tokyo

Sauter, C.; Lorber, B.; McPherson, A. & Giegé, R. (2011). Crystallization, In: *General methods In International Tables of Crystallography; Crystallography of Biological Macromolecules,* pp. In press., Chichester

Sazaki, G.; Moreno, A. & Nakajima, K. (2004). Novel coupling effects of the magnetic and electric fields on protein crystallization. *Journal of Crystal Growth*, Vol. 262, No. 1-4, pp. 499-502, ISBN 0022-0248

Schmolka, I. (1977). A review of block polymer surfactants. *Journal of the American Oil Chemists' Society*, Vol. 54, No. 3, pp. 110-116,

Sumner, J. (1926). The isolation and crystallization of the enzyme urease. Preliminary paper. *Journal of Biological Chemistry*, Vol. 69, No. 2, pp. 435-441,

Takáts, Z.; Vékey, K. & Hegedüs, L. (2001). Qualitative and quantitative determination of poloxamer surfactants by mass spectrometry. *Rapid Communications in Mass Spectrometry*, Vol. 15, No. 10, pp. 805-810,

Tardieu, A.; Le Verge, A.; Riès-Kautt, M.; Malfois, M.; Bonneté, F.; Finet, S. & Belloni, L. (1999). Proteins in solution : from X-ray scattering intensities to interaction potentials. *J. Crystal Growth*, Vol. 196, No. pp. 193-203, ISSN: 0022-0248

ten Wolde, P. R. & Frenkel, D. (1997). Enhancement of protein crystal nucleation by critical density fluctuations. *Science*, Vol. 277, No. pp. 1975-1978,

Tessier, P. M.; Vandrey, S. D.; Berger, B. W.; Pazhianur, R.; Sandler, S. I. & Lenhoff, A. M. (2002). Self-interaction chromatography: a novel screening method for rational protein crystallization. *Acta Cryst.*, Vol. D58, No. 10 Part 1, pp. 1531-1535, ISSN: 0907-4449

Vekilov, P. G. (2010). Nucleation. *Crystal Growth & Design*, Vol. 10, No. 12, pp. 5007-5019, WOS:000284675100001

Velev, O. D.; Kaler, E. W. & Lenhoff, A. M. (1998). Protein interactions in solution characterized by light and neutron scattering: comparison of lysozyme and chymotrypsinogen. *Biophys. J.*, Vol. 75, No. 6, pp. 2682-2697, ISSN: 0006-3495

Vérétout, F.; Delaye, M. & Tardieu, A. (1989). Molecular basis of eye lens transparency. Osmotic pressure and X-ray analysis of alpha-crystallin solutions. *J. Mol. Biol.*, Vol. 205, No. 4, pp. 713-728, ISSN: 0022-2836

Visuri, K.; Kaipainen, E.; Kivimaki, J.; Niemi, H.; Leisola, M. & Palosaari, S. (1990). A New Method for Protein Crystallization Using High Pressure. *Nature Biotechnology*, Vol. 8, No. 6, pp. 547-549,

Vivares, D. & Bonneté, F. (2002). X-ray scattering studies of Aspergillus flavus urate oxidase: towards a better understanding of PEG effects on the crystallization of large proteins. *Acta Cryst.*, Vol. D58, No. pp. 472-479, ISSN: 0907-4449

Vivares, D.; Astier, J.-P.; Veesler, S. & Bonnete, F. (2006). Polymorphism of urate oxidase in PEG solutions. *Crystal Growth & Design*, Vol. 6, No. pp. 287-292, ISSN: 1528-7483

Vivares, D.; Belloni, L.; Tardieu, A. & Bonneté, F. (2002). Catching the PEG-induced attractive interaction between proteins. *Eur. Phys. J. E.*, Vol. 9, No. pp. 15-25,

Weber, M.; Jones, M. J. & Ulrich, J. (2008). Crystallization as a Purification Method for Jack Bean Urease: On the Suitability of Poly(Ethylene Glycol), Li2SO4, and NaCl as Precipitants. *Cryst. Growth Des.*, Vol. 8, No. 2, pp. 711-716, ISBN 1528-7483

Wulff-Pérez, M.; Torcello-Gómez, A.; Gálvez-Ruíz, M. J. & Martín-Rodríguez, A. (2009). Stability of emulsions for parenteral feeding: Preparation and characterization of o/w nanoemulsions with natural oils and Pluronic f68 as surfactant. *Food Hydrocolloids*, Vol. 23, No. 4, pp. 1096-1102,

Ye, X.; Narayanan, T.; Tong, P.; Huang, J. S.; Lin, M. Y.; Carvalho, B. L. & Fetters, L. J. (1996). Depletion interactions in colloid-polymer mixtures. *Phys. Rev. E*, Vol. 54, No. 6, pp. 6500-6510, ISSN: 1063-651X

Zheng, B.; Gerdts, C. J. & Ismagilov, R. F. (2005). Using nanoliter plugs in microfluidics to facilitate and understand protein crystallization. *Current Opinion in Structural Biology*, Vol. 15, No. pp. 548–555, ISSN: 0959-440X

IntechOpen